Journal of Structural Geology 32 (2010) 151–165

Contents lists available at ScienceDirect

Journal of Structural Geology

journal homepage: www.elsevier.com/locate/jsg

Active fault and shear processes and their implications for mineral deposit formation and discovery

Steven Micklethwaite [a,*], Heather A. Sheldon [b], Timothy Baker [c]

[a] CODES, School of Earth Sciences, University of Tasmania, Private Bag 126, Hobart, TAS 7001, Australia
[b] CSIRO Exploration & Mining, PO Box 1130, Bentley, WA 6102, Australia
[c] Geological Survey of South Australia, GPO Box 1671, Adelaide, SA 5001, Australia

ARTICLE INFO

Article history:
Received 7 April 2009
Received in revised form
2 October 2009
Accepted 20 October 2009
Available online 28 October 2009

Keywords:
Fault and fluids
Epithermal
Lode gold
Carlin
Seismogenesis
Stress transfer
Damage mechanics
CO_2

ABSTRACT

Mineralisation associated with fault, vein and shear zone systems can be related to processes that operated when those systems were active. Despite the complexity of processes that operate in faults, veins and shear zones, there are typically systematic patterns in geometry (e.g. segmentation and step-overs) and scaling, which are the cumulative result of multiple slip events. In turn, there are systematic patterns in individual slip events (e.g. earthquake-aftershock sequences, shear zone creep transients, earthquake swarms) with implications for permeability enhancement and mineral deposit formation. This review identifies three avenues for future research: (1) a need to improve constraints on the scaling characteristics of faults, shear zones and veins specifically related to mineralisation. (2) The integration of stress change and damage concepts with 3-D lithological observations and reactive transport modelling. (3) Understanding the impact of multiphase fluids (e.g. H_2O–CO_2–NaCl fluids) on fault mechanics and permeability. Static stress change modelling, damage mechanics modelling and fault/vein scaling concepts have promising predictive capabilities for the future discovery of mineral deposits. The review mostly refers to epithermal, mesothermal, and carlin-type gold deposits, but the principles could extend to any hydrothermal mineral deposit formed during faulting, fracturing and shearing.

1. Introduction

A fundamental aim of structural analysis applied to mineralisation is to identify how deformation influenced the enhancement or decrease of permeability in rocks, both spatially and over time. During the last 20 years, structural investigations have recognized the important role of transient, repeated, earthquake-related processes, in enhancing permeability and forming mineral deposits (e.g. Sibson, 1987; Sibson et al., 1988; Robert et al., 1995; Wilkinson and Johnston, 1996; Berger and Drew, 2003; Blundell et al., 2003; Muchez et al., 2005; Micklethwaite and Cox, 2004). In the same period of time, advances in seismology and geodesy, have helped identify a rich diversity of processes that operate in faults and shear zones, which result in both seismic and aseismic behaviour (e.g. Scholz, 2002; Freed, 2005; Schwarz and Rokosky, 2007). Understanding this variety of behaviour can help us constrain where and how permeability was generated around fault or shear zone systems that are no longer active. Similarly, numerical models initially developed to understand active fault behaviour have the potential to be applied to mineral exploration (Micklethwaite, 2007; Sheldon and Micklethwaite, 2007).

Before this review proceeds it is necessary to define a few terms. Mineralisation is a broad term, referring to naturally occurring processes that concentrate inorganic substances, especially metal ores. Strictly, 'mineral deposit' or its synonym 'ore deposit' are economic terms, because they describe ores that are so concentrated that the economics of extraction are feasible. Structural geology does not aim to predict the concentration of ores and therefore cannot predict the location of mineral deposits. Nonetheless, by understanding the spacing, geometry, development and mechanics of potentially mineralised structures, structural geology is an invaluable tool to mineral exploration.

The first part of this paper briefly discusses the temporal variability of permeability and the relationship between permeability, faulting and shearing. The second part outlines the geometries and scaling properties of well-constrained fault, vein and shear zone systems, in the context of observations from ore deposits. These properties are the cumulative result of multiple slip and fracture events (such as earthquakes) and in turn geometric features (such as step-overs) control the distribution of slip events. The third part of the paper discusses aspects of active fault and shear zone behaviour that relate to mineralisation. The fourth part of the paper

* Corresponding author. Tel.: +61 3 6226 7208; fax: +61 3 6226 7662.
E-mail address: Steven.Micklethwaite@utas.edu.au (S. Micklethwaite).

0191-8141/$ – see front matter © 2009 Elsevier Ltd. All rights reserved.
doi:10.1016/j.jsg.2009.10.009

covers recent modelling approaches advancing our understanding of active faulting, and fluid flow, which are also directly applicable as mineral exploration tools. This final section considers the relationship between CO_2 and seismicity, and the influence of CO_2-bearing aqueous fluids on the mechanics of faulting during mineralisation.

Closely related reviews include the relationship between earthquake processes and structural geology (Sibson, 1989, 2001), and the driving forces for fluid flow and permeability enhancement during ore deposit formation at depth in the crust (Cox, 2005). Oliver (2001) discusses the migration of metamorphic fluids and formation of ore deposits in and around faults or shear zones, and Blundell (2002) examines the geodynamic context of ore deposits and how earthquake processes contribute to deposit formation.

2. Deformation, permeability and mineralisation in the crust

Geological structure has a first-order spatial relationship with hydrothermal ore deposits. Examples include greenstone-hosted lode gold deposits, which typically form at mid-crustal depths (Fig. 1), within damage zone faults and veins, adjacent to regional-scale master faults or shear zones (Eisenlohr et al., 1989; Cox et al., 1995; Robert et al., 2005; Micklethwaite and Cox, 2006). Similarly, Carlin-type gold deposits are spatially associated with large normal fault systems (Cline et al., 2005) within the top 2 km of the crust (Fig. 1). Many types of epithermal gold deposit (Hedenquist and Lowenstern, 1994) are hosted within vein or dilatant fault networks (Simmons et al., 2005; Micklethwaite, 2009) at depths of less than 1 km.

A one-to-one correlation between structure and hydrothermal ore deposits is understandable when the metal budgets of deep hydrothermal solutions are examined, such as those from the geothermal environments of the Taupo Volcanic Zone, New Zealand (Simmons and Brown, 2007). The flux of gold and silver in solution (80–163 and 6800–13,850 kg Ag/yr) could easily account for the formation of the worlds largest hydrothermal ore deposits in a short time period of ~50,000 years. However, no deposits have been discovered in the Taupo Volcanic Zone, leading Simmons and Brown (2007) to conclude the most important processes for deposit formation are focussed fluid flow and efficient metal precipitation. Focussed fluid flow in particular is dependent on changes in permeability in and around structures, over time.

2.1. Permeability

Permeability is a measure of the ease with which fluid migrates through porous rock (Domenico and Schwarz, 1998). Permeability is not a material property but a parameter, dependent on hydraulic gradient and the physical or chemical controls affecting the porosity (Cox, 2005). In and around fault and shear systems, permeability is typically time-dependent, due to competition between various chemical and physical processes, as illustrated in Fig. 2.

Three important conclusions emerge from studies of fault, vein and shear zone related permeability. (1) Deformation can enhance permeability by many orders of magnitude. (2) Permeability can rapidly decrease post-slip or fracture. (3) Small components of structural networks in the brittle upper crust have elevated values of permeability, which persist over extended periods of time. Generally though, the formation of fault-related hydrothermal mineral deposits requires active deformation in order to sustain elevated values of permeability and enable focussed fluid flow. Evidence for these conclusions, permeability magnitudes and rates of decrease are outlined below.

2.2. Permeability and rates of variation

Permeability within fault zones potentially varies over ten orders of magnitude, from bulk rock values of $\sim 10^{-20}$ to $>10^{-16}$ m^2 (Manning and Ingebritsen, 1999; Townend and Zoback, 2000), up to co-seismic and postseismic values estimated at 10^{-13} to 10^{-11} m^2 (Koerner et al., 2004; Miller et al., 2004).

Rates of permeability reduction in fault gouges have been quantified by hydrothermal deformation experiments (e.g. Tenthorey et al., 2003; Tenthorey and Fitz Gerald, 2006; Giger et al., 2007; Kay et al., 2006), generally at high temperatures or specific fluid compositions, in order to enhance kinetics. The studies of Tenthorey and Fitz Gerald (2006), and Kay et al. (2006) are noteworthy because they involved reasonable crustal temperatures of 200–600 and 120 °C, respectively. Permeability decreases due to redistribution of material

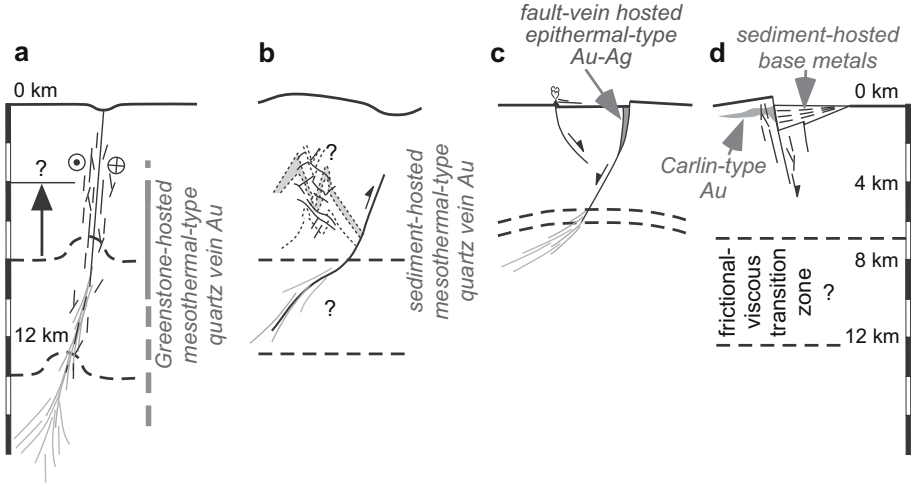

Fig. 1. Schematic diagram illustrating the approximate depths and structural environments interpreted for a small selection of different deposit types. (a) Mesothermal lode gold mineralisation associated with regional-scale strike-slip shear zones (e.g. Robert et al., 2005). (b) Mesothermal lode gold mineralisation hosted in veins within folded turbiditic sediments, associated with steep reverse dip faulting. (c) Fault or vein-hosted epithermal gold mineralisation. (d) Carlin-type gold mineralisation typically associated with large-scale normal dip-slip faults, close to the surface (Cline et al., 2005). Regional-scale structures in mesothermal environments are typically phyllosilicate-rich. Phyllosilicate-bearing fault rocks and/or slightly elevated geothermal gradients and could lead to shallow depths for the frictional–viscous transition zone, of ~5 km (Imber et al., 2001).

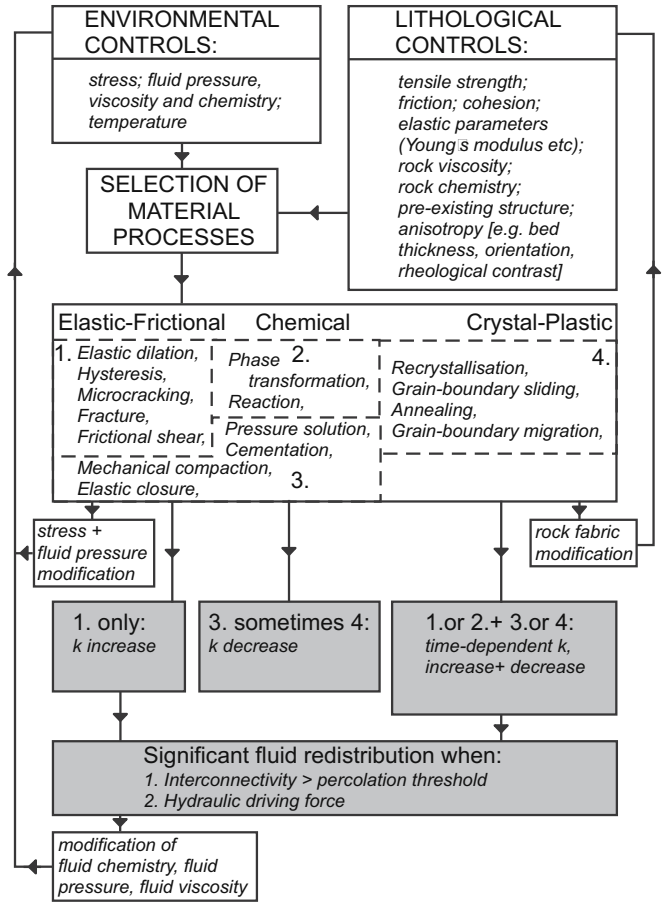

Fig. 2. Flow diagram outlining the set of controlling variables and inter-relationships between deformation, alteration and fluid interaction. See Knipe (1989) for a summary of the environmental and lithological controls that influence material processes and rock deformation in isolation.

and sealing of the gouge (e.g. by pressure dissolution and local deposition of the dissolved material; path 3 in Fig. 2). Extrapolations to natural systems indicate an order of magnitude decrease in permeability is achieved, within days to years after a fault slip event. Fracture-sealing experiments similarly indicate rapid sealing within hours under experimental conditions, in both quartz and calcite materials (Hickman and Evans, 1987; Brantley et al., 1990). Experimental constraints on the sealing rates are still required for variations in fluid salinity, pH and aperture size (Brantley et al., 1990).

In natural systems after large earthquakes, outflows measured from springs and rivers, hydrogeochemical monitoring of groundwater aquifers (Rojstaczer et al., 1995; Claesson et al., 2007), and geophysical observations of changing seismic wave properties (e.g. Tadokoro and Ando, 2002; Hiramatsu et al., 2005), all suggest large co-seismic permeability enhancement, typically followed by the healing of fault and fracture planes within 2–3 years. Importantly, in geothermal conditions analogous to the formation of vein-hosted epithermal deposits, silica cementation occurs rapidly at shallow crustal levels (e.g. Clark and Williams-Jones, 1990). Under these conditions, effective fluid focussing is critically reliant on active deformation to enhance permeability, which subsequently decreases due to cementation and mechanical compaction processes (paths 1 and 3, Fig. 2). Thus fluid flow related to active fault systems is likely to be episodic. Indeed, Fig. 3 documents the geometries and textures of "fault-valve" structures typically found hosting ore in mesothermal lode gold deposits (e.g. Sibson et al., 1988; Boullier and Robert, 1992; Cox, 1995; Kolb et al., 2004; Micklethwaite, 2008). These belong to a class of fault process that could be referred to as *dilational faulting* (Ferrill and Morris, 2003), which is likely to be effective at focussing fluid flow. Multiple overprinting breccia textures and crack-seal vein textures imply repeated episodes of seismic rupture then sealing (Sibson et al., 1988; Boullier and Robert, 1992; Woodcock et al., 2007).

2.3. Persistence of elevated permeability

Drill core sampling of the San Andreas Fault system ($\leq$3.5 km depth) found a small percentage of faults and fractures remain open to migrating fluids (Barton et al., 1995). These fractures were optimally oriented, i.e. the orientations of the conductive fractures is such that they would be the most likely to fail first given the orientation of the prevailing stress field. Barton et al., (1995), interpreted these fractures to be "critically stressed", assuming the fractures were cohesionless with friction values of 0.6–1.0. Fairley and Hinds (2004), using measurements of spring water temperatures along a left-stepping en echelon fault system, concluded the fault is presently characterised by low permeability values but contains spatially discrete high-permeability channels. Thus a small proportion of fault-enhanced permeability appears to persist over extended periods of time (path 1 in Fig. 2).

2.4. Permeability and mid-crustal shear zones

At mid-crustal depths, elastic closure, cementation, or temperature-activated crystal-plastic deformation processes begin to dominate deformation (e.g. ~300 °C for quartzo-feldspathic rocks), acting to maintain permeability at low values in wall rock volumes (paths 3 and 4, Fig. 2). However, within shear zones, significant permeability enhancement still occurs during creep. This is achieved by the generation of grain boundary or intragranular microcracks during creep (McCaig and Knipe, 1990; Géraud et al., 1995; Peach and Spiers, 1996; Bauer et al., 2000). Additionally, as shear zones undergo crystal-plastic deformation, fluid is trapped in migrating grain boundary pores, (e.g. cavitation; Mancktelow et al., 1998; Rybacki et al., 2008), or migrates through tubular porosity at grain–grain junctions and within certain mineral phases (e.g. microcracks and tubules more readily formed in feldspar; Géraud et al., 1995). As will be shown later in this paper, shear zone creep can undergo repeated high strain rate transients, thus shear zone fluid localisation may be episodic in the mid-lower crust as with faults in the upper crust.

2.5. Implications of episodic permeability variation

The episodic nature of structure-related mineral systems is an important conclusion. Cox (2007) measured oxygen and carbon isotope compositions from individual increments of calcite veins, contained in a deformed limestone sequence. The structural style is analogous to mesothermal lode gold deposits in folded sedimentary sequences (e.g. Fig. 1), such as Bendigo goldfield in Victoria, Australia. Isotope compositions were fluid buffered from the earliest increments of vein formation, they varied from increment to increment and they described a sharp oxygen isotope front, higher in the limestone sequence, which did not migrate with time. This suggests episodic pulses of fluid flow occurred, where during each increment, fluids escaped from an external reservoir and accessed slightly different fracture pathways. Each fluid pulse becoming rock buffered at broadly the same structural level (Cox, 2007). The results imply that continuum models of deformation, fluid flow and mineralisation, with progressively advancing alteration fronts through homogenous fault zones, are not applicable to problems of mineral deposit formation when episodic fluid flow is involved.

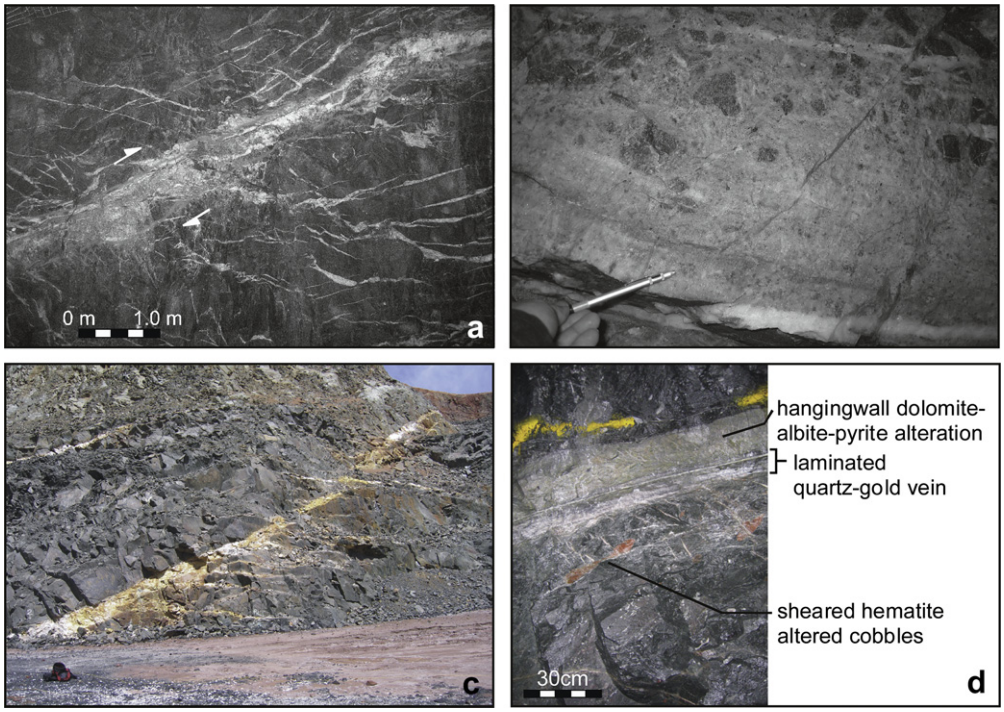

Fig. 3. Photos of "fault-valve" reverse-slip structures (Sibson et al., 1988) associated with mesothermal gold mineralisation, from three different gold deposits, West Australia. The textures indicate dilatant faulting, and repeated episodes of highly focussed fluid flow. (a, b) Reverse-slip fault with a central extensional-shear vein, containing layers of cement-supported breccia, indicating multiple episodes of slip and cementation. Linked and unlinked arrays of extension veins are mutually overprinting in the hangingwall and footwall. Argo gold deposit, St Ives. (c) Thrust fault with an extensional-shear vein linked to footwall and some hangingwall extension veins. Rucksack for scale. Triumph deposit, New Celebration (modified from Micklethwaite, 2008). (d) A laminated vein with asymmetric hangingwall alteration halo, and a damage zone of small extensional-shear veins that offset cobbles in the host rock. Wallaby deposit, Laverton (modified from Micklethwaite, 2007).

3. Structural architecture of mineral deposits

Systematic patterns exist in the geometry (e.g. step-overs and segmentation) and scaling properties of structural systems, which are also common to structures associated with mineral deposits (Fig. 4).

3.1. Scaling

Key attributes of a structural system are the scaling relationships of the system. Scaling relationships are interdependent relationships between frequency, displacement, length, connectivity, thickness, spacing, etc., which have been found to exist in well-constrained fossil and active systems. They are the cumulative result of seismic and aseismic processes operating during fault and fracture growth (e.g. Cowie and Scholz, 1992; Cowie et al., 1995; Cowie, 1998; Walsh et al., 2003), which control the growth, linkage and/or branching of structures. The scaling properties of faults and fractures, and the complications that surround this issue, are thoroughly reviewed by Bonnet et al. (2001).

Because scaling relationships identify systematic patterns to structural systems they are potentially useful for mineral deposit exploration. For instance, scaling studies have been applied to mineralised vein systems with some success; to understand the growth, connection and percolation of fluids through Sn–W vein systems (Roberts et al., 1999; Foxford et al., 2000; Sanderson et al., 2008), the probability of intersecting gold-bearing veins at depth (McCaffrey and Johnston, 1996), and the influence of different lithologies on the spacing and thickness of epithermal Au–Ag veins (Brathwaite et al., 2001).

In active fault systems, displacement-length scaling relationships have been used to constrain the across-strike spacing of structures (Cowie and Roberts, 2001; Soliva and Benedicto, 2005). This approach could be adapted to estimate across-strike spacing of structures in mineralised systems and generate tools for predictive mineral exploration, but the work remains to be done. Indeed, recent detailed studies have identified a distinction between *distributed-type* and *localised-type* fault systems (Soliva and Schultz, 2008), with implications for the prediction of fault spacing. Localised-type fault systems have self-similar scaling properties and contain linked and unlinked faults, with strain coalesced on a few large structures (Soliva and Schultz, 2008). In contrast, distributed-type fault systems comprise nearly regular across-strike spacing of faults with small relative displacement (e.g. Soliva and Benedicto 2005), potentially because the faults are restricted by the thickness of a rock layer during growth (Soliva and Schultz, 2008). Figs. 4a and 5a show the Cracow epithermal goldfield, Queensland, Australia, and Acupan epithermal goldfield, Philippines, respectively. Strain is coalesced into a few larger structures similar to a localised-type fault system, thus predicting the location and spacing of structures would require a scaling approach. Against this, the structure of other epithermal deposits (e.g. Martha Hill, New Zealand) can be more mesh-like and regularly spaced (Fig. 5b), similar to distributed-type systems, and suggesting a more straight-forward predictability to structure location under cover.

Currently, little is known about the scaling properties of dilational faults, that seem to be so important for mesothermal lode gold deposit formation (Fig. 3; Sibson et al., 1988; Cox, 1995; Kolb et al., 2004; Micklethwaite, 2008), and epithermal deposits (Dreier, 2005; Nortje et al., 2006; Begbie et al., 2007; Micklethwaite, 2009). Approaches utilizing scaling properties can be complicated in mineral deposit studies because faults and shear zones localise on pre-existing fabrics, or have multiple phases of activation (e.g. Carlin deposits, Muntean et al., 2007; mesothermal deposits, Weinberg et al., 2005).

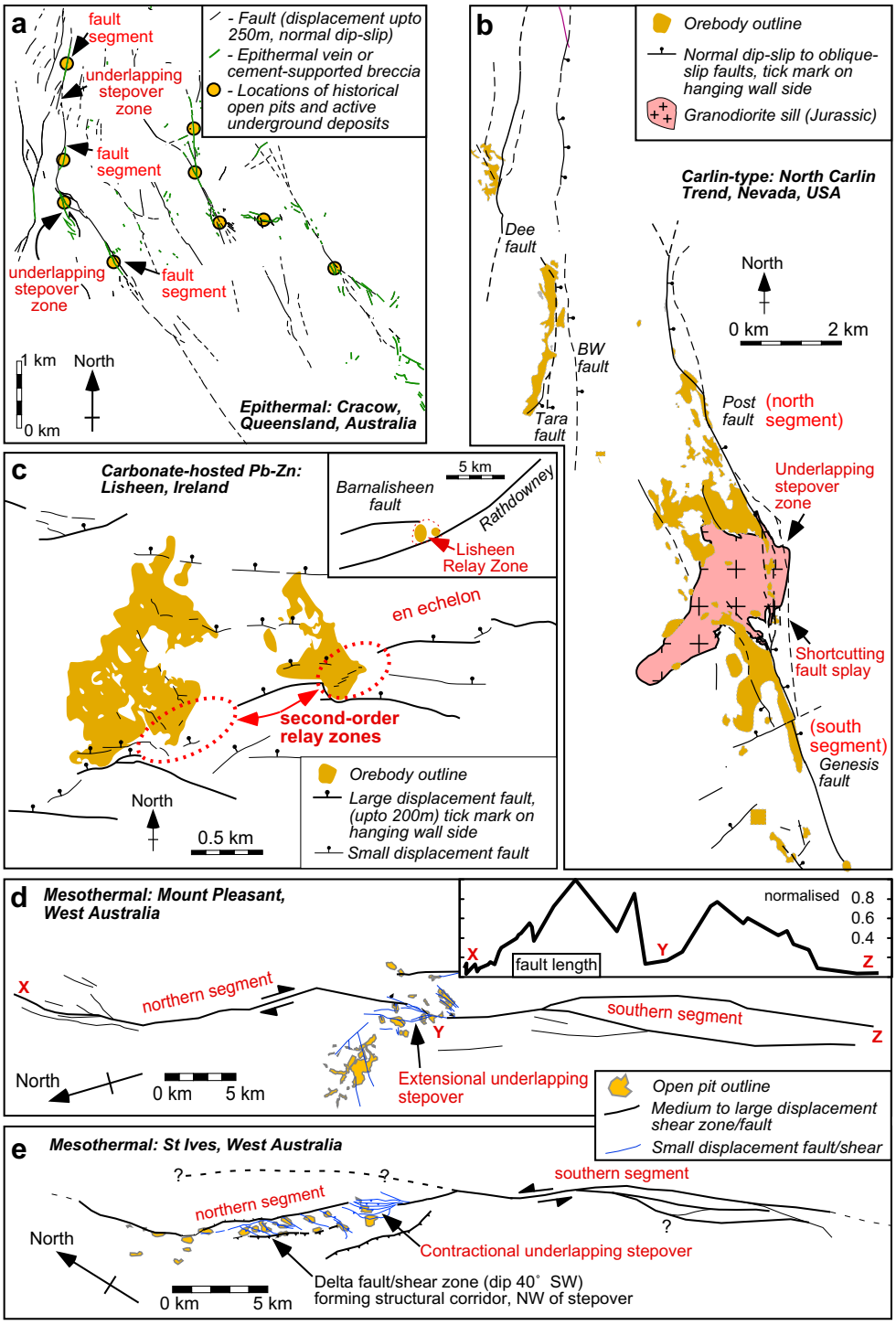

Fig. 4. Structural maps of different fault and shear zone systems associated with mineralisation. The systems all display typical features such as segmentation, development of step-overs and branching at fault tips. (a) Cracow epithermal goldfield, Australia (modified from Micklethwaite, 2009). This is an example of a localised-type epithermal fault system where strain is coalesced into one to two large structures. The larger structures appear to comprise multiple segments and step-overs (labelled). (b) North Carlin trend goldfield, U.S.A. (compiled from Nevada Bureau of Mines and Geology Bulletin 111, 2002). The Post-Genesis fault system is two segments, separated by an underlapping stepover zone. Majority of mineralisation is close to and distributed laterally away from the stepover. (c) Lisheen Pb–Zn base metal deposit, Ireland (modified from Hitzman et al., 2002; Carboni et al., 2003). The Rathdowney and Barnalishee faults are interpreted as large single segments at depth (inset), forming multiple en echelon segments at shallower levels. Mineralisation is spatially associated with two different scales of stepover; the Lisheen relay between the two faults, and smaller second-order relays developed along the Rathdowney fault. (d, e) Mesothermal gold deposits, West Australia (modified from Micklethwaite and Cox, 2006). Mineralisation is spatially associated with and distributed laterally away from step-overs. In contrast, mineralisation at Cracow has no spatial relationship with a single fault location type but occurs at step-overs, fault segments and tip zones.

3.2. Segmentation and step-overs

Arguably the two most important geometric elements of fault, shear zone and vein systems for mineralisation are *segmentation*, and the development of *step-overs* between segments (sometimes referred to as jogs). Segments are relatively continuous sections of a structure that localise displacement, then tend to bifurcate into arrays of smaller structures or fracture networks towards their tips

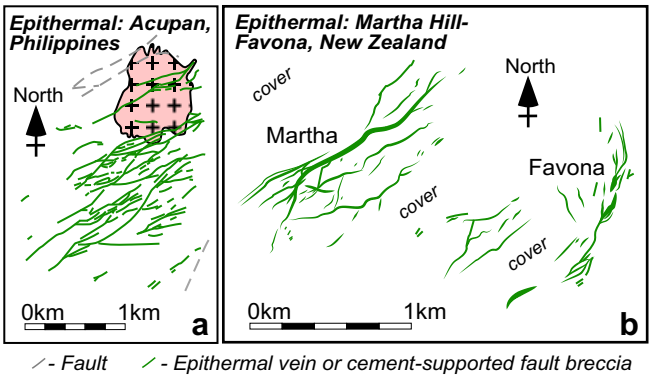

Fig. 5. Distributed epithermal veins systems. (a) Acupan, and (b) Martha Hill. Martha Hill displays a semi-regular spacing, which is not apparent in the Cracow goldfield (Fig. 4a). Modified from Torkler et al. (2006) and the compilation in Simmons et al. (2005).

(see the excellent study by Kim et al., 2003). Faults and veins typically comprise multiple segments that interact with or link adjacent segments, across step-overs (e.g. see annotations in Fig. 4a). The step-overs represent zones of more distributed strain, typically containing second-order structures such as branch faults, fracture networks or folding (Pachell and Evans, 2002). Minima in fault displacement or vein thickness values occur at step-overs (e.g. Fig. 4d inset) when these quantities are traced along a structure (Ellis and Dunlap, 1988; Peacock, 1991; Peacock and Sanderson, 1991; Pachell and Evans, 2002), although minima tend to disappear when bedding rotation or displacements on the full fracture network are accounted for at step-overs (Walsh et al., 2003). Segmentation can also be observed at multiple scales. Second-order variations in the displacement profile of the Black Flag fault (Fig. 4d inset) suggest the two large segments of the Black Flag fault are themselves composed of smaller segments.

There are three important attributes of step-overs describing the nature of their linkage, geometry and strain field (Fig. 6). (1) Segments are *hard-linked* across step-overs by branch fault or fracture networks. Alternatively they are *soft-linked* when a component of strain is accommodated by bed rotation or folding, and there is no through going fracture network. (2) Segments *overlap* or *underlap* across step-overs, defined by the location of the tips of the bounding segments relative to each other (Fig. 6a; Aydin and Schultz, 1990; Childs et al., 1995; Acocella et al., 2000). (3) Step-overs are "*contractional*" or "*extensional*" steps, depending on the dominant strain field in the stepover controlled by the shear sense on the adjacent segments (Fig. 6b; Kim et al., 2003). Step-overs or jogs are alternatively referred to as restraining and releasing, or compressional and dilational.

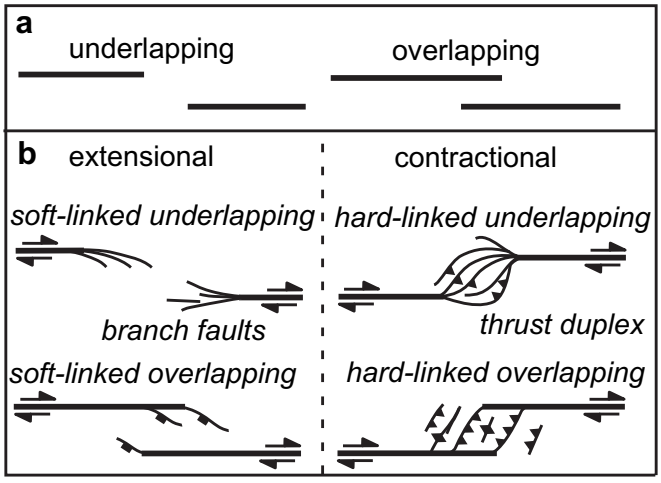

Fig. 6. Summary of attributes and features associated with step-overs on fault or shear zone systems.

Segmentation has been proposed to explain the spacing of mineral deposit clusters along structural systems (Micklethwaite, 2007), such as is observed with mesothermal gold deposits (Robert and Poulsen, 1997; Weinberg et al., 2004; Robert et al., 2005). Fig. 4 shows fault and shear zone controlled mineral deposits correlated with segments and step-overs. Carlin-type gold, greenstone-hosted mesothermal gold and Pb–Zn mineralisation are associated with step-overs on large-scale faults (Fig. 4b–e). The step-overs are both contractional and extensional steps. Mesothermal mineralisation specifically is hosted in, or associated with, small-displacement structures, some of which link across the step-overs (Fig. 4d,e). Pb–Zn mineralization at Lisheen (Fig. 4c and inset) has an association with soft-linkage between en echelon fault segments.

The influence of segmentation and step-overs on mineralisation does not appear to be limited by depth. For instance, the Carlin-type Au deposits associated with a stepover in Fig. 4b formed at >2 km depth (Cline et al., 2005), whereas the mesothermal Au deposits of Fig. 4d,e typically form at mid-crustal depths (McCuaig and Kerrich, 1998) adjacent to regional-scale shear zones. Critically, mineralisation is distributed beyond the step-overs shown in Fig. 4, occupying significant surface areas of 4–15 km^2. Thus step-overs are a locus for, but not a limit to mineralisation.

4. Seismic and aseismic processes and fluid redistribution

Active fault and geothermal systems are natural laboratories for understanding mineralisation processes, and seismological or geodetic studies are instructive in helping us understand how fracture and shear zone related porosity is enhanced within the crust.

Deformation is achieved by a variety of modes of behaviour in active systems. These include earthquakes triggering clusters of aftershocks, or further earthquakes, on adjacent faults (e.g. Reasenberg and Simpson, 1992; Stein et al., 1992; Stein et al., 1997; Freed, 2005), intrusion events triggering earthquake swarms (Fukuyama et al., 2001; Toda et al., 2002), aseismic upper crust fault creep or mid-crust shear zone creep plus associated microseismicity, slow-slip and non-volcanic tremor (Freed, 2005; Schwartz and Rokosky, 2007). Useful regions for studying seismic and aseismic behaviour are well-constrained continental fault systems such as the San Andreas Fault, USA, as well as active geothermal regions like North Island, New Zealand, or Long Valley Caldera, USA.

4.1. Earthquakes and aftershocks

Fig. 7 shows aftershock distributions for three well-constrained earthquake rupture traces – 1992 M_W7.3 Landers earthquake, USA, the 1999, M_L7.6 Izmit earthquake, North Anatolian fault, Turkey and the 1986 M_L5.7 Mount Lewis earthquake, USA. Firstly, aftershocks form clusters, especially around the tips and step-overs of fault segments. In long-section and map-view, aftershocks tend to cluster around the perimeters of rupture surfaces (e.g. Cakir et al., 2003). Secondly, the clusters can be spread over distances greater than 10 km from the master fault (Fig. 7a).

Another consideration is the scaling relationship between seismic magnitude and frequency (Gutenberg–Richter relationship) within a region and even within a single earthquake-aftershock sequence,

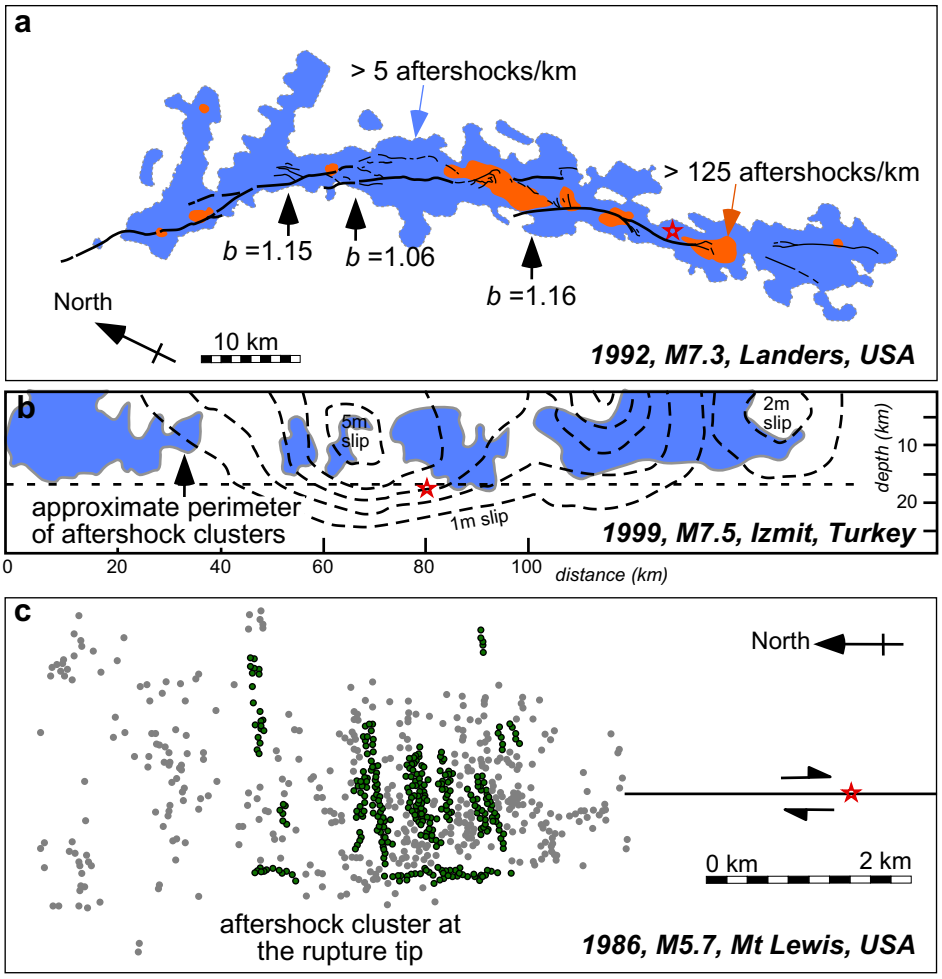

Fig. 7. (a) Map of the Landers earthquake surface rupture trace and contours of aftershock density, modified from Liu et al., (2003). High aftershock density, and frequency (*b*-values >1.0) correlates with step-overs and bends on the fault trace. (b) Long-section projection of the slip distribution of the Izmit earthquake (dashed contours) compared with the approximate outline of aftershock clusters (blue) with $M_L \geq 2$, modified from model III of Çakir et al. (2003). Aftershock clusters tend to form around the perimeter of the rupture plane. Aftershocks are mostly confined to the upper crust (<16 km, dotted horizontal line), but the mainshock nucleated and propagated below the seismic–aseismic transition (>20 km). (c) Map-view of high resolution relocations of aftershocks, which form a cluster in the tip zone of the Mount Lewis rupture. Aftershocks selected in green define distinct linear trends indicating multiple reactivation of the same fault planes. Modified from Kilb and Rubin (2002).

$$\log_{10} N = a - b\mathrm{M} \quad (1)$$

where *N* is the number of earthquakes in a sequence with magnitudes greater than or equal to M, while *a* and *b* are constants (with the latter referred to as the *b*-value). The *b*-value is large when there are high frequencies of small earthquakes. Typically, *b*-values cluster around unity, ranging from 0.7 to 1.3 (Frohlich and Davis, 1993). Because Eq. (1) is a power-law relationship, even small differences in *b* represent large differences in the intensity of fracturing experienced after an earthquake.

4.1.1. Step-overs and fracture frequency

Segment tips and step-overs are important geometric barriers and control the nucleation and arrest of earthquakes (Sibson, 1985; Wesnousky, 1988; Kase and Kuge, 1998; Wesnousky, 2006). Step-overs also correlate with regions of high *b*-value, following large earthquakes. Liu et al. (2003) mapped aftershock density recorded around the 1992 M_W7.3 Landers earthquake and found that high *b*-values (1.00–1.16) occurred at step-overs and bends in surface rupture traces (Fig. 7a). The Landers rupture typifies many large earthquakes, in that it was able to jump across fault step-overs and continue propagating. Commonly, during large earthquakes, this occurs when co-seismic slip decreases abruptly towards the step-over (Elliott et al., 2009). The stepover itself is not breached, and the strain that is transferred to the stepover region is then released by high frequencies of aftershocks (high *b*-values). Once the distance to the next fault segment exceeds 3–4 km, the geometric barrier represented by fault step-overs prevents jumping or propagation of a fault rupture (Wesnousky, 2006).

The observation that high *b*-values (>1.0) are encountered in stepover regions, when slip events jump or arrest at those step-overs, is important for stepover related mineral deposits (e.g. Fig. 4). High *b*-values indicate there is a high density of aftershocks and a high degree of connectivity generated in such regions, per earthquake sequence. In this regard accurate relocations of aftershocks give an indication of the density and connectivity that occurs per sequence. A good example is the 1986 M_L5.7 Mount Lewis earthquake (Kilb and Rubin, 2002). Here aftershocks localised on the same secondary faults, repeatedly within the one sequence (Fig. 7c). This means that even in one earthquake-aftershock sequence, elevated values of permeability can be maintained on aftershock-hosting faults for extended periods of time, with persistent reactivation of the same structures (Fig. 7c).

Many fault or shear zone related mineral deposits are hosted by or associated with secondary structures with 0.1–1 km length

(e.g. Robert et al., 1995; Micklethwaite and Cox, 2004, 2006). It is possible to use Eq. (1), and empirical relationships between earthquake magnitude and fault length (c.f. Well and Coppersmith, 1994) to estimate the number of rupture events of similar dimension within a single earthquake sequence (Fig. 8). For the mesothermal lode gold Val d'Or district (Abitibi, Canada), Robert et al. (1995) suggested the extensional-shear veins, which host the gold, were activated as aftershocks, in the range $3 < M < 4$ on the basis of the average slip surface. In the case where a master segment ruptures during a M6 event, aftershock domains with *b*-values greater than unity (e.g. $b = 1.2$) host ~250 events that rupture 1 km-long fault lengths (~M4), and ~4000 events repeatedly reactivate 300 m-long patches of faults (~M3 in Fig. 8).

4.2. Earthquakes and shear zone creep

The depth range over which seismicity exerts its influence is mostly confined by the thickness of the brittle upper crust. The main parameter that controls this thickness is temperature (Sibson, 1983; Scholz, 2002), whereby the seismic–aseismic transition coincides with the frictional–viscous transition due to the onset of crystal-plastic deformation mechanisms at depth. In continental regions, the seismic–aseismic transition is estimated from background microseismicity to occur at 10–15 km. In geothermal regions, with elevated geothermal gradients in the order 50–100 °C, the seismic–aseismic transition occurs as shallow as 4–6 km (e.g. Bryan et al., 1999; Reyners et al., 2007).

However there are important exceptions to this general rule, as indicated by Fig. 7b, where the Izmit earthquake nucleated at 16 km and propagated to >20 km depth. Very large earthquakes therefore, have the ability to puncture the frictional–viscous transition and fracture portions of the system normally undergoing shear zone creep. Large earthquakes are also able to trigger aftershocks at depth, which then shallow over time (Fig. 9). Rolandone et al. (2004) analysed the 1992 M_W7.3 Landers earthquake and statistically defined the seismic–aseismic transition as the depth above which 95% of earthquakes occurred. With this approach, they demonstrated that aftershocks were triggered 10–15 km below the long-term seismic–aseismic transition, that the seismic–aseismic transition deepened by 3–4 km and that the transition then shallowed by 3 km over the next 4 years (Fig. 9). Presumably co-seismic stress, transferred from Landers earthquake, exceeded the Coulomb shear strength of deeper rocks normally undergoing shear zone creep, and they were temporarily subject to brittle failure.

Stress transfer not only triggers brittle failure events but also increases shear zone creep rates. Large earthquakes within the seismogenic upper crust increase static stress on shear zones at depth, and trigger viscous creep at high strain rates, that decays over months to years (Ellis and Stöckhert, 2004; Johnson and Segall, 2004). Evidence for high strain rate creep events is given by quartz microstructures from exhumed shear zones (e.g. Trepmann and Stöckhert, 2003), and GPS measurements of the velocity field around transcrustal fault systems (e.g. Savage et al., 2003; Johnson and Segall, 2004; Montési, 2004). The shear zones may be mylonitic continuations of the earthquake-hosting fault, or they may be separate structures at moderately large lateral distances to the mainshock fault (c.f. Freed and Lin, 2001; Pollitz and Sacks, 2002). Brittle fracturing can also nucleate at or below the brittle–ductile transition due to the aggregation of cavities or highly deformed feldspars (Rybacki et al., 2008; Shigematsu et al., 2009).

The likely outcome of this behaviour is that fluid flow in shear zones has a large episodic component, just as with seismogenic fault systems in the upper crust, due to: (1) high strain rate creep transients resulting from earthquake stress transfer; and (2) downward propagation of large earthquakes and concomitant fracturing. A matter yet to be resolved is whether shear zone hosted mineral deposits are more dependent on these episodic permeability enhancement processes, or long-term creep and permeability.

4.3. Earthquakes in geothermal environments

Geothermal regions, in particular, are environments where epithermal deposits form (Clark and Williams-Jones, 1990; Simmons et al., 2005). Fault failure in geothermal environments can be very dynamic, involving both typical earthquake-aftershock sequences and earthquake swarms (e.g. Taupo Volcanic Zone, Hurst

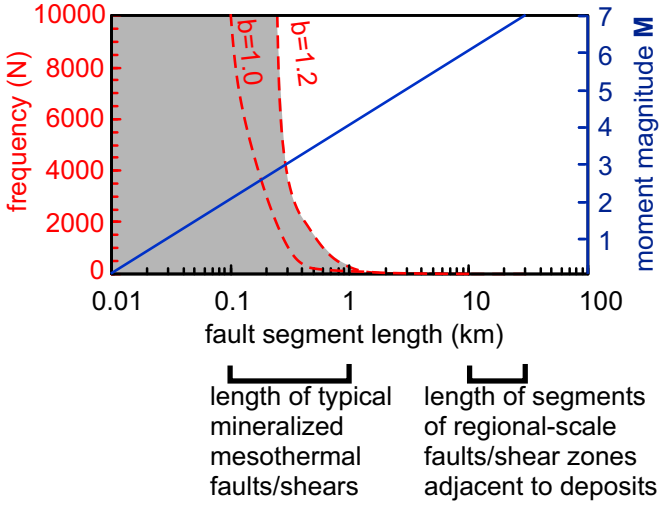

Fig. 8. Combined frequency-length and length-magnitude plot showing two relationships. In blue is the empirical relationship between earthquake magnitude and the length of a ruptured segment (e.g. Table 1 of Sibson, 1989; Wells and Coppersmith, 1994). Regional-scale mesothermal shear zones tend to have segments 10–30 km. In red, is the scaling relationship between aftershock frequency and fault length, derived for faults that may be expected to be triggered as aftershocks (faults <1 km length), following a M6 mainshock event on a mesothermal shear zone segment (*b*-values >1.0 are associated with aftershocks around step-overs and fault tips).

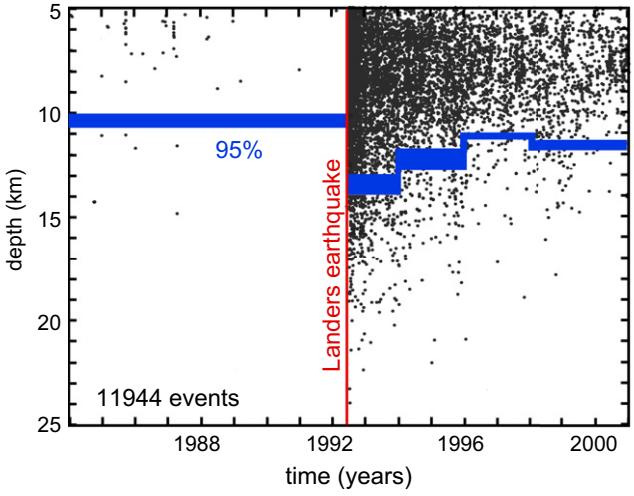

Fig. 9. The time and depth distribution of seismic events prior to and following the Landers M_W7.3 earthquake. The blue line shows the depth above which 95% of earthquakes occur, which is a widely used measure of the seismic–aseismic transition. Its variation is shown for different time windows (June 28 1992–1994, 1994–1996, 1996–1998, 1998–2001). Modified from Rolandone et al. (2004).

et al., 2008). Earthquake swarms tend to have high frequencies of earthquakes (high *b*-value), with slow development of seismicity and no clear hierarchy between the larger and smaller events. Earthquake swarms are of great interest because of the potential for sustained permeability enhancement implied by large densities of earthquakes closely located in space and time (e.g. >16,000 events, *b*-values up to 1.5; Jenatton et al., 2007).

Earthquake swarms are triggered by geological events that induce small changes in local stress state. These include the intrusion of dikes (Fukuyama et al., 2001; Toda et al., 2002; Waite and Smith, 2002), or oscillations induced by the passage of seismic waves from distant large earthquakes (Hill et al., 1993, 1995; Husen et al., 2004; Brodsky and Prejean, 2005). Failure events were triggered in the Yellowstone National Park by the Alaskan Denali M7.9 earthquake, >3000 km away (Husen et al., 2004). The small stress changes involved suggests faults in these environments are close to failure.

One explanation for the critical failure state of geothermal faults is elevated pore fluid pressure (Hill et al., 1993). Indeed, the impact of fluid pressure on fault-fracture mechanics is significant for mineralisation of structures in fluid-saturated hydrothermal regimes, at all crustal depths. Fluid pressure reduces rock strength and induces fracturing or shear failure according to the effective stress law, whereby fluid pressure (P_f) reduces any normal stress (σ_{ij}) transmitted between rock particles. Since fluid pressure acts equally in all directions it does not effect shear stress components (e.g. $\sigma'_{ij} = \sigma_{ij} - P_f\delta_{ij}$, where δ_{ij} is the Kronecker delta, which is 1 if $i = j$, but 0 otherwise). By this mechanism elevated fluid pressures in fractures or intergranular porosity can maintain faults at stress levels close to their failure strength. Sibson (2001) presents a good introduction to tectonic stress and fluid pressure affects.

Evidence for elevated pore fluid pressures in geothermal environments comes from non-double-couple earthquake focal mechanisms (Dreger et al., 2000) – that is earthquake mechanisms resolved on faults that involve extensional-shear failure (Dreger et al., 2000; Foulger et al., 2004; Templeton and Dreger, 2006). Non-double-couple earthquakes occur as microseismicity (Foulger et al., 2004), but also as M3–4 events (Templeton and Dreger, 2006), involving rupture of ~300–1000 m of fault length (Fig. 8). The larger magnitude events represent a small percentage of the total seismicity across the region and occur over a range of depths (1.5–8 km). Because confining pressures encountered at such depths are large, elevated fluid pressures are necessary to explain extensional-shear failure and are likely to be important in the triggering of non-double-couple failure events. By implication, these earthquakes may be the origin of some dilational fault type epithermal deposits (Micklethwaite, 2009), and are thought to be accompanied by aqueous or CO_2-rich fluids flowing into open fractures.

5. Influence of stress changes, damage and fluid chemistry on faulting, fluid flow and mineralisation

5.1. Triggers for seismicity-dynamic and static stress changes, and stress transfer modelling

There are a variety of physical mechanisms responsible for the triggering of aftershocks after an earthquake. During and immediately after the mainshock, changes in static stress are imposed on the rocks around the rupture (Reasenberg and Simpson, 1992; Stein et al., 1992; Voisin et al., 2004; Freed, 2005), while seismic and shock waves radiated by the earthquake induce transient dynamic stress changes (Gomberg et al., 2001, 2004; Voisin et al., 2004; Brodsky and Prejean, 2005; Bouchon and Karabulut, 2008). These static and dynamic stress changes influence the distribution of aftershocks. After the mainshock, time-dependent processes can additionally influence aftershock distribution. These include viscoelastic creep of the lower crust, transferring stress back to the upper crust (Freed, 2005), release of a pulse of overpressured fluids from a fluid reservoir (Koerner et al., 2004; Miller et al., 2004), or relaxation of co-seismic changes in pore fluid pressure (Shapiro et al., 2003; Antonioli et al., 2005). Nonetheless, in the near-field of the mainshock (first 10–15 km), static stress changes commonly have a first-order control over the distribution of aftershocks (Hardebeck et al., 1998; Gomberg et al., 2001; Voisin et al., 2004), and these stress changes can be calculated using a method known as stress transfer modelling (STM; King et al., 1994). Static stress changes appear to be important for both earthquake-aftershock sequences, and for earthquake swarms triggered by intrusion of dykes (e.g. Toda et al., 2002; Roman and Cashman, 2006). Static stress changes are also generated by faults during aseismic slip events, such as frictional creep.

STM calculates Coulomb failure stress ($\Delta\sigma_f$) around a fault, represented in 3-D as an elastic dislocation. Importantly, STM is relatively straight-forward and has been applied to mineralised faults in the rock record (Cox and Ruming, 2004; Micklethwaite and Cox, 2004, 2006). STM operates by relating changes in shear stress ($\Delta\tau_f$) and normal stress ($\Delta\sigma_n$), to changes in Coulomb failure stress,

$$\Delta\sigma_f = \Delta\tau + \mu'(\Delta\sigma_n) \quad (2)$$

The apparent coefficient of friction (μ') ranges from 0.2 to 0.8 (see King et al., 1994; Cox and Ruming, 2004; Micklethwaite and Cox, 2006). Most other input parameters are simple and readily attained from field data, such as fault shape, the orientation of the regional stress field, fault slip direction and estimates of approximate slip magnitude from fault segment length (see Fig. 8 for the empirical relationship between segment length and magnitude). Modelling can be done rapidly, with freely available software (e.g. GNStress or COULOMB, http://quake.wr.usgs.gov/research/deformation/modeling/coulomb/index.html). Micklethwaite and Cox (2006) applied STM to demonstrate a close correlation between the distribution of mesothermal gold deposits, and domains where faults and shears are expected to be triggered by earthquakes on master faults (Fig. 10a,b).

The utility of STM for exploration is immediately obvious from Fig. 10a,b. Maps or 3-D images (Fig. 10c–e) of positive stress change can be generated and used to inform exploration drilling programs, or identify new areas worth targeting. The technique is particularly useful where the distribution of historic mining provides an additional partial constraint. The results are also invaluable from a theoretical perspective because they suggest the dominant process controlling fluid redistribution around mid-crustal faults and shear zones is stress triggered fracturing in the damage zones of the master structures.

In Fig. 10c–e, we illustrate 3-D change in Coulomb failure stress around three different types of fault, 10 × 10 km in dimension (a normal fault, a right-lateral strike-slip fault and a reverse dip-slip fault with a 60° dip). The distributions of positive static stress changes at 0.05 and 0.2 MPa are shown. In all cases positive stress changes are generated in cylinder-like domains around the perimeter of the master slip, suggesting that damage and permeability enhancement can be triggered at distances of 2 to >5 km away from the master slip. For each fault type, the stress changes penetrate deeper than the triggering rupture, connecting to the surface through vertical, continuous domains. Comparisons between the models indicate there are similar dimensions to the positive stress domains, and by extension similar dimensions to that portion of damage zone that would be activated by each fault type during a slip event. The strike-slip fault triggers stress changes

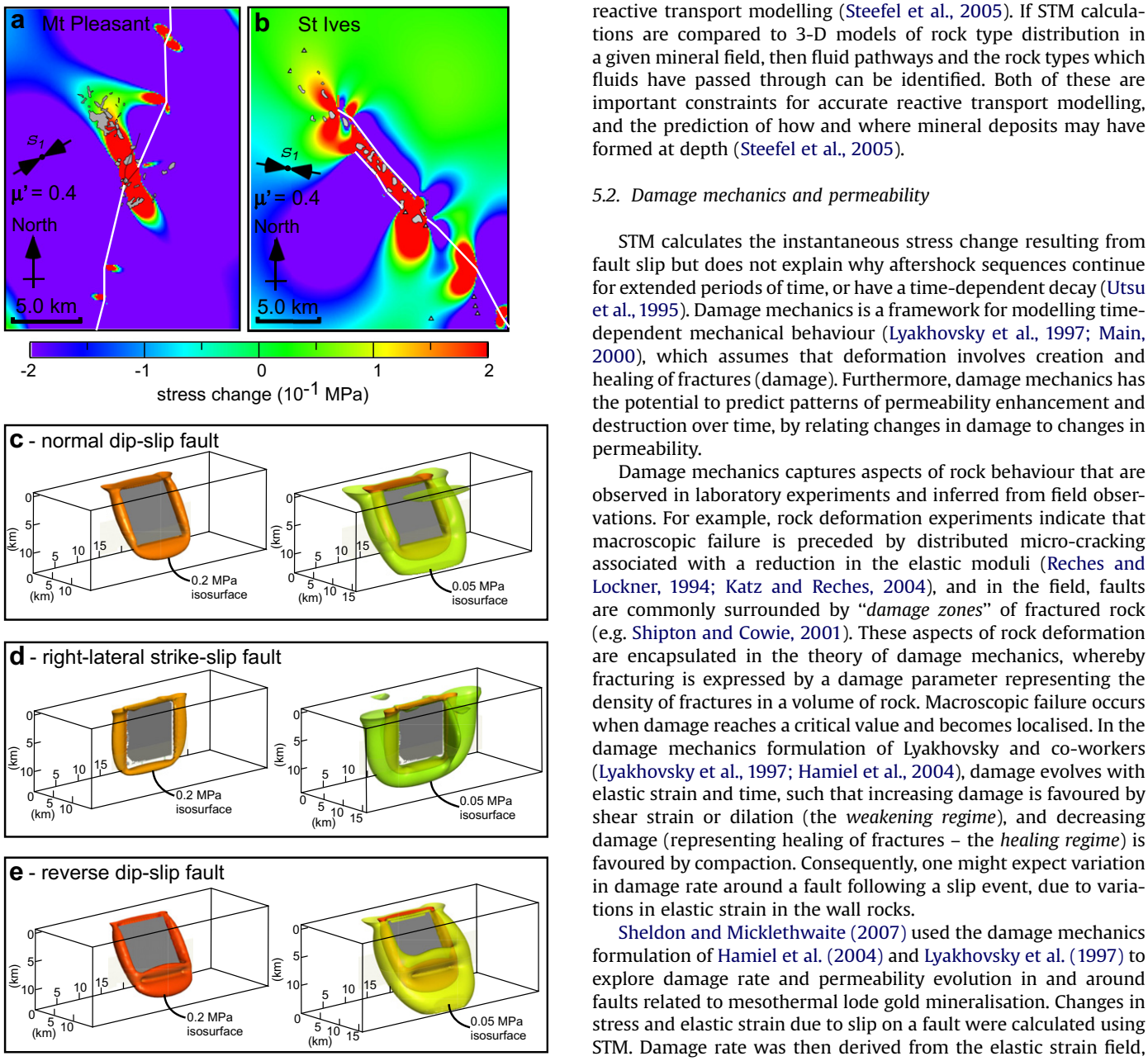

Fig. 10. (a, b) Combined-slip stress transfer calculations from the Mount Pleasant and St Ives mesothermal goldfields. The distribution of mineral deposits (gray polygons) matches the distribution of positive Coulomb failure stress change around paleoslip events on the major faults in these goldfields (see Micklethwaite and Cox, 2006, for details). S1 is the direction of maximum compressive stress imposed on the models. (c–e) Comparison between 3-D stress change isosurfaces for (c), a normal dip-slip fault, (d) a right-lateral strike-slip fault, (e) a reverse dip-slip fault, with dip angle of 60°, which is typical for some mesothermal lode gold deposits (e.g. Sibson, 2001). The isosurfaces represent Coulomb failure static stress changes at 0.2 and 0.05 MPa, respectively. Each model superimposes the same far-field stress magnitude (100 MPa differential stress) and the fault surfaces have the same dimensions (10 × 10 km). For purposes of comparison, each model has a uniform slip distribution of 0.4 m. The dimensions and slip are equivalent to a M6 earthquake.

over larger lateral distances, especially along strike of the master fault (Fig. 10d) but the normal and reverse dip-slip faults (Fig. 10c,e, respectively) trigger stress changes to greater depths (>5 km below the base of the rupture surface) and therefore have potential to tap deeper fluid reservoirs.

3-D calculations of stress transfer are promising for mineral deposit studies because of their potential to be combined with reactive transport modelling (Steefel et al., 2005). If STM calculations are compared to 3-D models of rock type distribution in a given mineral field, then fluid pathways and the rock types which fluids have passed through can be identified. Both of these are important constraints for accurate reactive transport modelling, and the prediction of how and where mineral deposits may have formed at depth (Steefel et al., 2005).

5.2. Damage mechanics and permeability

STM calculates the instantaneous stress change resulting from fault slip but does not explain why aftershock sequences continue for extended periods of time, or have a time-dependent decay (Utsu et al., 1995). Damage mechanics is a framework for modelling time-dependent mechanical behaviour (Lyakhovsky et al., 1997; Main, 2000), which assumes that deformation involves creation and healing of fractures (damage). Furthermore, damage mechanics has the potential to predict patterns of permeability enhancement and destruction over time, by relating changes in damage to changes in permeability.

Damage mechanics captures aspects of rock behaviour that are observed in laboratory experiments and inferred from field observations. For example, rock deformation experiments indicate that macroscopic failure is preceded by distributed micro-cracking associated with a reduction in the elastic moduli (Reches and Lockner, 1994; Katz and Reches, 2004), and in the field, faults are commonly surrounded by "*damage zones*" of fractured rock (e.g. Shipton and Cowie, 2001). These aspects of rock deformation are encapsulated in the theory of damage mechanics, whereby fracturing is expressed by a damage parameter representing the density of fractures in a volume of rock. Macroscopic failure occurs when damage reaches a critical value and becomes localised. In the damage mechanics formulation of Lyakhovsky and co-workers (Lyakhovsky et al., 1997; Hamiel et al., 2004), damage evolves with elastic strain and time, such that increasing damage is favoured by shear strain or dilation (the *weakening regime*), and decreasing damage (representing healing of fractures – the *healing regime*) is favoured by compaction. Consequently, one might expect variation in damage rate around a fault following a slip event, due to variations in elastic strain in the wall rocks.

Sheldon and Micklethwaite (2007) used the damage mechanics formulation of Hamiel et al. (2004) and Lyakhovsky et al. (1997) to explore damage rate and permeability evolution in and around faults related to mesothermal lode gold mineralisation. Changes in stress and elastic strain due to slip on a fault were calculated using STM. Damage rate was then derived from the elastic strain field, assuming that the master fault underwent a stress drop at the time of the slip event, such that deviatoric stress in the fault was temporarily reduced to zero following the slip event. In this scenario, the pattern of damage rate in the wall rocks is very similar to the pattern of $\Delta\sigma_f$ predicted by STM. In other words, areas of positive damage rate correspond closely to areas where aftershocks and mineralisation are expected to be triggered by static stress changes.

One of the key results to emerge from the approach of Sheldon and Micklethwaite (2007) is that the master fault enters the healing regime following the fault slip event, due to stress drop and consequent mechanical compaction. Therefore permeability changes associated with damage evolution in and around the fault permits a larger fluid flux to pass through the aftershock zones than through the master fault itself. These results provide an explanation for the lack of gold mineralisation in the master faults and shear zones of mesothermal lode gold goldfields. We hypothesise that areas of positive damage rate (i.e. aftershock zones, or areas brought closer to failure as a consequence of fault slip) correlate

with mineralisation, because these are the only places where permeability can be sustained while minerals are precipitating (c.f. Micklethwaite and Cox, 2004).

Much remains to be done in applying damage mechanics to mineral deposit studies or exploration. Well-constrained algorithms linking damage to permeability are yet to be developed but percolation approaches offer promise. For example, Souley et al. (2001) linked permeability to crack connectivity by comparing laboratory measurements of permeability in granite with in situ hydraulic tests. A second aspect that should be considered is the effect of chemical reactions on permeability (e.g. Tenthorey and Fitz Gerald, 2006). Permeability reduction due to mineral precipitation might help us understand why, in some circumstances, the larger ore deposits in a goldfield are distributed away from master faults and step-overs, rather than immediately adjacent to the master fault where the greatest damage (and therefore the greatest permeability enhancement) is expected. Combining damage mechanics with reactive transport modelling would help us understand these issues.

Finally, relationships between faulting, fracturing and permeability evolution appear to differ between different deposit types. Carlin-type and mesothermal lode gold mineralisation can be related to damage and step-overs adjacent to large faults or shear zones (e.g. Figs. 4 and 10). In contrast, vein-hosted epithermal deposits are hosted in the master structures themselves, possibly due to much larger components of dilatancy during faulting at shallow depths (Micklethwaite, 2009). Other deposit types, such as porphyry Cu–Au, are hosted in intrusives that are sometimes located in step-overs along regional-scale strike-slip fault systems (e.g. Garza et al., 2001; Richards, 2003), although this correlation remains poorly constrained. In this latter case, the critical relationship to investigate is that between stepover or fault tip damage, permeability evolution and the migration of viscous magmatic fluids.

5.3. Exploring the role of multiphase fluids (e.g. H_2O–CO_2–NaCl)

Crustal hydrothermal fluids commonly contain one or more volatile components, such as CO_2, in addition to water. The presence of CO_2 in ore-forming fluids has long been known from fluid inclusion studies (e.g. mesothermal – Wilkinson and Johnston, 1996; McCuaig and Kerrich, 1998; epithermal – Simmons et al., 2005). More recent work has identified the role of CO_2-bearing fluids in triggering slip and fracture events in modern fault systems. For example, high fluxes of CO_2 have been measured close to earthquake swarms (Bräuer et al., 2008) and there is a strong correspondence between seismicity and overpressured fluid reservoirs containing CO_2 in Italy (Chiodini et al., 2004; Miller et al., 2004; Bonini, 2009) and elsewhere (Irwin and Barnes, 1980). Colletini et al. (2006) and Smith et al. (2008) implicated CO_2-bearing fluids in slip on low-angle normal faults and the formation of vein networks and breccias. In geothermal environments, CO_2-rich fluids are responsible for the formation of travertine and consequent sealing of faults (Hancock et al., 1999; Uysal et al., 2007).

The significance of volatile components in crustal fluids lies in the physical and chemical changes that occur when the fluid crosses the boundary between one-phase and two-phase conditions in P–T space. For example, faulting drives phase separation by generating rapid fluid pressure drops. Indeed, this process could relate to the precipitation of some gold in mesothermal lode gold deposits (e.g. Sibson et al., 1988; McCuaig and Kerrich, 1998) by triggering changes in fluid pH and sulphur fugacity at the phase boundary. Here, we consider the influence of faulting on phase separation, but also explore the possibility that phase separation itself drives fault failure – namely faulting triggered by fluid pressure increase as the rock resists expansion of the fluid phase at the phase boundary.

Fig. 11 illustrates a phase boundary for a H_2O–CO_2–NaCl fluid composition typical of mesothermal gold systems ($XCO_2 = 0.12$; $XH_2O = 0.86$; $XNaCl = 0.02$; e.g. McCuaig and Kerrich, 1998; Ridley and Diamond, 2000). A single liquid phase exists in the one-phase field, which separates into a vapour phase plus a liquid phase on crossing the boundary into the two-phase field. The shaded area in Fig. 11 indicates the typical range of P–T conditions for the formation of mesothermal lode gold deposits (~1–2.5 kbars, and ~250–350 °C), although some deposits extend the range further (e.g. Val d'Or, Abitibi, ~3.5 kbars and 350 °C; Boullier and Robert, 1992; Robert et al., 1995). Notice the broad coincidence between this shaded area and the location of the phase boundary, suggesting a link between phase separation and mesothermal gold mineralisation.

The black dot in Fig. 11 represents an overpressured fluid (i.e. a fluid at lithostatic pressure) at 8 km depth, with a temperature representative of a reasonable Archaean geothermal gradient (50 °C/km; e.g. Goscombe et al., 2007). Three possible P–T evolution pathways are shown for the fluid, representing common geological processes. The isobaric path represents cooling at constant pressure, such as may occur close to a cooling intrusion. The molar volume of the fluid increases from ~27 to ~48 cm^3 on crossing the phase boundary along this path, representing a 78% increase in fluid volume (volumes calculated using the equation of state from Duan et al., 1995; available at http://geotherm.ucsd.edu/geofluids/run_geofluids1.cgi). Similarly, an overpressured fluid cooling along a geothermal gradient of 50 °C/km, e.g. due to erosion, experiences a fluid volume increase from ~33 to ~50 cm^3 at the phase boundary (51% volume increase). In scenarios where the rock fails to accommodate these large changes in fluid volume, there must be an increase in fluid pressure at the phase boundary, which in turn may cause reactivation of existing faults, veins or shear

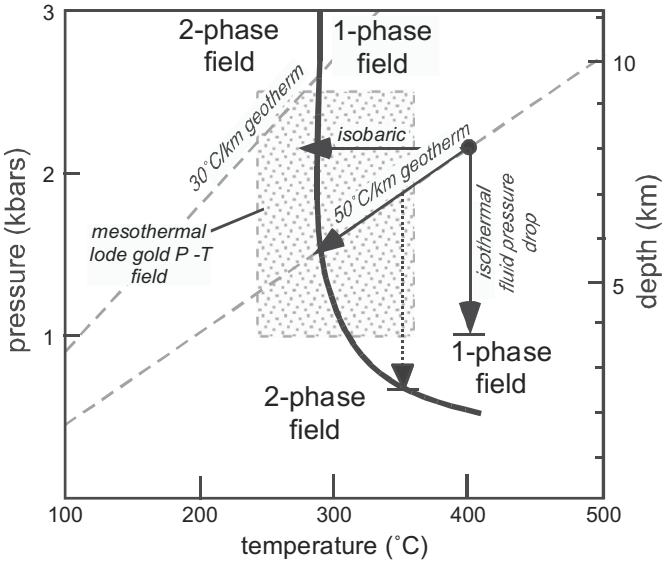

Fig. 11. Pressure-temperature-depth plot illustrating the relationship between the phase boundary for a typical mesothermal lode gold fluid (H_2O–CO_2–NaCl) and the P–T conditions associated with mesothermal gold fields (McCuaig and Kerrich, 1998). Phase equilibria and volumetric properties were calculated using an equation of state for H_2O–CO_2–NaCl (Duan et al., 1995; http://geotherm.ucsd.edu/geofluids/run_geofluids1.cgi). Arrows indicate P–T paths that a mid-crustal fluid could travel during a few earthquake cycles (isobaric, isothermal, and evolving along a geothermal gradient). Drop in fluid pressure along the isothermal paths was estimated on the basis of a lithostatically pressured fluid reservoir becoming connected with a hydrostatically pressured fluid column.

zones and/or formation of new structures. In particular, the concept that cooling could lead to the nucleation of earthquakes by fluid pressure increase in fluid reservoirs, would seem to be a counter-intuitive but important result. The focussing of cooling fluids along reactivated structures may explain some earthquake swarms.

The isothermal path in Fig. 11 represents a drop in fluid pressure from lithostatic to hydrostatic, such as might occur when rupture events on faults or shear zones breach an overpressured fluid reservoir. This path does not cross the phase boundary. However, a similar fluid pressure drop at slightly shallower depth (~7 km; dashed arrow in Fig. 11) would intersect the phase boundary, with a very large molar volume increase from ~36 to ~98 cm^3 (172% volume increase). Notice that this second isothermal path coincides with the upper temperature boundary of the mesothermal gold ore-forming conditions (shaded area in Fig. 11). In other words, ~350 °C is the maximum temperature at which an isothermal pressure drop triggered by fault failure would intersect the phase boundary, and this is also the general upper limit of temperatures associated with mesothermal gold mineralisation. Fluid inclusion studies have previously suggested a relationship between veins subject to large fluid pressure drops and the spatial distribution of gold mineralisation (Wilkinson and Johnston, 1996).

It is interesting to consider what happens when the isothermal path intersects the phase boundary, because the fluid pressure drop will be offset by the fluid pressure increase associated with phase change. The isothermal path will only cross the phase boundary (to lower pressure) if the fluid pressure increase due to phase change is insufficient to offset the fluid pressure drop. Further investigation is required to compare the magnitudes of the fluid pressure changes associated with fault failure and phase change, and to understand the consequences for fluid flow and mineralisation.

In conclusion, we have identified several geological processes which could cause a typical mesothermal gold fluid to cross from the one-phase field into the two-phase field. This in turn has consequences for fault reactivation, fluid flow and mineralisation. Phase separation is dependent on fluid composition and not just P–T conditions, so that for example a fluid with higher XCO_2 may undergo phase separation at higher P–T conditions. Thus the impact of CO_2 on fault mechanics may vary from the shallow crust to granulite facies conditions in relation to faults and shear zones.

6. The future

The review presented above highlights three avenues of research that are important to the future understanding of mineral deposit formation and discovery:

(1) Improving constraints on the scaling properties of faults, veins and shear zones, which are specifically related to mineral deposits. Scaling properties have potential application to issues such as the prediction of the spacing of lodes, or the development of new exploration drilling strategies.
(2) Combining stress transfer modelling and damage mechanics with reactive transport modelling to understand where and how mineralisation is likely to occur.
(3) Assessment of the impact of the phase separation of volatile-bearing fluids on fault reactivation, permeability enhancement and fluid flow.

Acknowledgements

Thorough reviews by B. Berger and A.-M. Boullier, and the editorial assistance of J.Hippertt are gratefully acknowledged. Matt Crawford is thanked for permission to publish a photo from Argo gold deposit, where he is conducting a postgraduate research. Stephen Cox was previously an excellent mentor and originally introduced S.M. to the implications of active fault processes and experimental observations for mineral deposit formation. This paper was possible due to the support and access over the years provided by AMIRA International, Barrick Gold, Harmony, Gold Fields, Placer Dome, Newmont, AngloGold-Ashanti, KCGM and Newcrest. Some of the concepts in this paper were developed when S.M. was at the Australian National University under Australian Research Council Linkage grants LP0218720 and LP0562164, awarded to Stephen Cox.

References

Acocella, V., Gudmundsson, A., Funiciello, R., 2000. Interaction and linkage of extension fractures and normal faults: examples from the rift zone of Iceland. Journal of Structural Geology 22, 1233–1246.
Antonioli, A., Piccinini, D., Chiaraluce, L., Cocco, M., 2005. Fluid flow and seismicity pattern: evidence from the 1997 Umbria-Marche (central Italy) seismic sequence. Geophysical Research Letters 32, 1–4. doi:10.1029/2004GL022256. L10311.
Aydin, A., Schultz, R.A., 1990. Effect of mechanical interaction on the development of strike-slip faults with echelon patterns. Journal of Structural Geology 12, 123–129.
Bauer, P., Palm, S., Handy, M.R., 2000. Strain localization and fluid pathways in mylonite: inferences from in situ deformation of a water-bearing quartz analogue (norcamphor). Tectonophysics 320, 141–165.
Barton, C.A., Zoback, M.D., Moos, D., 1995. Fluid flow along potentially active faults in crystalline rock. Geology 23, 683–686.
Begbie, M.J., Spörli, K.B., Mauk, J.L., 2007. Structural evolution of the Golden Cross epithermal Au–Ag deposit, New Zealand. Economic Geology 102, 873–892.
Berger, B.R., Drew, L.J., 2003. Mineral-deposit models – new developments. In: Fabbri, A.G., Gaal, G., McCammon, R.B. (Eds.), Deposit and Geoenvironmental Models for Resource Exploitation and Environmental Security. Nato Science Series, Partnership Sub-Series 2: Environmental Security, vol. 80, pp. 121–134.
Blundell, D.J., 2002. The timing and location of major ore deposits in an evolving orogen: the geodynamic context. In: Blundell, D.J., Neubauer, F., von Quadt, A. (Eds.), The Timing and Location of Major Ore Deposits in an Evolving Orogen. Geological Society, London, Special Publication, vol. 204, pp. 1–12.
Blundell, D.J., Karnkowski, P.H., Alderton, D.H.M., Oszczepalski, S., Kucha, H., 2003. Copper mineralization of the Polish Kupferschiefer: a proposed basement fault-fracture system of fluid flow. Economic Geology 98, 1487–1495.
Bonnet, E., Bour, O., Odling, N.E., Davy, P., Main, I., Cowie, P., Berkowitz, B., 2001. Scaling of fracture systems in geological media. Reviews of Geophysics 39, 347–383.
Bonini, M., 2009. Structural controls on a carbon dioxide-driven mud volcano field in the Northern Apennines (Pieve Santo Stefano, Italy): relations with pre-existing steep discontinuities and seismicity. Journal of Structural Geology 31, 44–54.
Bouchon, M., Karabulut, H., 2008. The aftershock signature of supershear earthquakes. Science 320, 1323–1325. doi:10.1126/science.1155030.
Boullier, A.-M., Robert, F., 1992. Palaeoseismic events recorded in Archaean gold-quartz vein networks, Val d'Or, Abitibi, Quebec, Canada. Journal of Structural Geology 14, 161–179.
Brantley, S.L., Evans, B., Hickman, S.H., Crerar, D.A., 1990. Healing of microcracks in quartz: implications for fluid flow. Geology 18, 136–139.
Brathwaite, R.L., Cargill, H.J., Christie, A.B., Swain, A., 2001. Lithological and spatial controls on the distribution of quartz veins in andesite- and rhyolite-hosted epithermal Au–Ag deposits of the Hauraki Goldfield, New Zealand. Mineralium Deposita 36, 1–12.
Brodsky, E.E., Prejean, S.G., 2005. New constraints on mechanisms of remotely triggered seismicity at Long Valley Caldera. Journal of Geophysical Research 110, B04302. doi:10.1029/2004JB003211.
Bryan, C.J., Sherburn, S., Bibby, H.M., Bannister, S.C., Hurst, A.W., 1999. Shallow seismicity of the central Taupo Volcanic Zone, New Zealand: its distribution and nature. New Zealand Journal of Geology and Geophysics 42, 533–542.
Çakir, Z., de Chabalier, J.-B., Armijo, R., Meyer, B., Barka, A., Peltzer, G., 2003. Coseismic and early post-seismic slip associated with the 1999 Izmit earthquake (Turkey), from SAR interferometry and tectonic field observations. Geophysical Journal International 155, 93–110.
Carboni, V., Walsh, J.J., Stewart, D.R.A., Güven, J.F., 2003. Timing and geometry of normal faults and associated structures at the Lisheen Zn–Pb deposit, Ireland – investigating their role in the transport and trapping of metals. In: Eliopoulos, D.G. (Ed.), Proceedings of the Seventh Biennial SGA Meeting – Mineral Exploration and Sustainable Development. Millpress Science Publishers, Rotterdam, pp. 665–668.
Childs, C., Watterson, J., Walsh, J.J., 1995. Fault overlap zones within developing normal fault systems. Journal of the Geological Society of London 152, 535–549.

Chiodini, G., Cardellini, C., Amato, A., Boschi, E., Caliro, S., Frondini, F., Ventura, G., 2004. Carbon dioxide Earth degassing and seismogenesis in central and southern Italy. Geophysical Research Letters 31, L07615. doi:10.1029/2004GL019480.

Claesson, L., Skelton, A., Graham, C., Mörth, S.-M., 2007. The timescale and mechanisms of fault sealing and water-rock interaction after an earthquake. Geofluids 7, 427–440.

Clark, J.R., Williams-Jones, A.E., 1990. Analogues of epithermal gold-silver deposition in geothermal well scales. Nature 346, 644–645.

Cline, J.S., Hofstra, A.H., Muntean, J.L., Tosdal, R.M., Hickey, K.A., 2005. Carlin-type gold deposits in Nevada: critical geological characteristics and viable models. In: Economic Geology 100th Anniversary Volume, pp. 451–484.

Colletini, C., De Paola, N., Goulty, N.R., 2006. Switches in the minimum compressive stress direction induced by overpressure beneath a low-permeability fault zone. Terra Nova 18, 224–231.

Cowie, P.A., 1998. A healing-reloading feedback control on the growth rate of seismogenic faults. Journal of Structural Geology 20, 1075–1087.

Cowie, P.A., Roberts, G.P., 2001. Constraining slip rates and spacings for active normal faults. Journal of Structural Geology 23, 1901–1915.

Cowie, P., Scholz, C.H., 1992. Physical explanation for the displacement-length relationship of fault using a post-yield fracture mechanics model. Journal of Structural Geology 14, 1133–1148.

Cowie, P.A., Sornette, D., Vanneste, C., 1995. Multifractal scaling properties of a growing fault population. Geophysical Journal International 122, 457–469.

Cox, S.F., 1995. Faulting processes at high fluid pressures: an example of fault valve behavior from the Wattle Gully Fault, Victoria, Australia. Journal of Geophysical Research 100, 12841–12859.

Cox, S.F., 2005. Coupling between deformation, fluid pressures and fluid flow in ore-producing hydrothermal systems at depth in the crust. In: Economic Geology 100th Anniversary Volume, pp. 1–35.

Cox, S.F., 2007. Structural and isotopic constraints on fluid flow regimes and fluid pathways during upper crustal deformation: an example from the Taemus area of the Lachlan Orogen, SE Australia. Journal of Geophysical Research 112, 1–23. doi:10.1029/2006JB004734. B08208.

Cox, S.F., Ruming, K., 2004. The St Ives mesothermal gold system, Western Australia – a case of golden aftershocks? Journal of Structural Geology 26, 1109–1125.

Domenico, P.A., Schwarz, F.W., 1998. Physical and Chemical Hydrogeology. John Wiley & Sons, New York.

Dreger, D.S., Tkalcic, H., Johnston, M., 2000. Dilational processes accompanying earthquakes in the Long Valley Caldera. Science 288, 122–125.

Dreier, J.E., 2005. The environment of vein formation and ore deposition in the Purisima-Colon vein system, Pachuca Real del Monte District, Hidalgo, Mexico. Economic Geology 100, 1325–1347.

Duan, Z., Moller, N., Weare, J., 1995. Equation of state for NaCl–H_2O–CO_2 system – prediction of phase equilibria and volumetric properties. Geochimica Cosmochimica Acta 59, 2869–2882.

Eisenlohr, B.N., Groves, D., Partington, G.A., 1989. Crustal-scale shear zones and their significance to Archean gold mineralization in Western Australia. Mineralium Deposita 24, 1–8.

Elliott, A.J., Dolan, J.F., Oglesby, D.D., 2009. Evidence from coseismic slip gradients for dynamic control on rupture propagation and arrest through stepovers. Journal of Geophysical Research 114, 1–8. doi:10.1029/2008JB005969. B02312.

Ellis, M.A., Dunlap, W.J., 1988. Displacement variation along thrust faults: implications for the development of large faults. Journal of Structural Geology 10, 183–192.

Ellis, S., Stöckhert, B., 2004. Elevated stresses and creep rates beneath the brittle-ductile transition caused by seismic faulting in the upper crust. Journal of Geophysical Research 109, 1–10. doi:10.1029/2003JB002744. B05407.

Fairley, J.P., Hinds, J.J., 2004. Rapid transport pathways for geothermal fluid in an active Great Basin fault zone. Geology 32, 825–828. doi:10.1130/G20617.1.

Ferrill, D.A., Morris, A.P., 2003. Dilational normal faults. Journal of Structural Geology 25, 183–196.

Foulger, G.R., Julian, B.R., Hill, D.P., Pitt, A.M., Malin, P.E., Shalev, E., 2004. Non-double-couple microearthquakes at Long Valley caldera, California, provide evidence for hydraulic fracturing. Journal of Volcanology and Geothermal Research 132, 45–71.

Foxford, K.A., Nicholson, R., Polya, D.A., Hebblethwaite, R.P.B., 2000. Extensional failure and hydraulic valving at Minas da Panasqueira, Portugal: evidence from vein spatial distributions, displacements and geometries. Journal of Structural Geology 22, 1065–1086.

Freed, A.M., 2005. Earthquake triggering by static, dynamic, and postseismic stress transfer. Annual Reviews Earth and Planetary Science Letters 33, 335–367. doi:10.1146/annurev.earth.33.092203.122505.

Freed, A.M., Lin, J., 2001. Delayed triggering of the 1999 Hector Mine earthquake by viscoelastic stress transfer. Nature 411, 180–183.

Frohlich, C., Davis, S.C., 1993. Teleseismic *b* values; or, much ado about 1.0. Journal of Geophysical Research 98, 631–644.

Fukuyama, E., Kubo, A., Kawai, H., Nonomura, K., 2001. Seismic remote monitoring of stress field. Earth. Planets and Space 53, 1021–1026.

Garza, R.A.P., Titley, S.R., Pimentel, F., 2001. Geology of the Escondida porphyry copper deposit, Antofagasta Region, Chile. Economic Geology 96, 307–324.

Géraud, Y., Caron, J.-M., Faure, P., 1995. Porosity network of a ductile shear zone. Journal of Structural Geology 17, 1757–1769.

Giger, S.B., Tenthorey, E., Cox, S.F., Fitz Gerald, J.D., 2007. Permeability evolution in quartz fault gouges under hydrothermal conditions. Journal of Geophysical Research 112, B07202. doi:10.1029/2006JB004828.

Gomberg, J., Reasenberg, P.A., Bodin, P., Harris, R.A., 2001. Earthquake triggering by seismic waves following the Landers and Hector Mine earthquake. Nature 411, 462–464.

Gomberg, J., Bodin, P., Larson, K., Dragert, H., 2004. Earthquake nucleation by transient deformations caused by the M = 7.9 Denali, Alaska, earthquake. Nature 427, 621–624.

Goscombe, B., Blewett, R., Czarnota, K., Maas, R., Groenewald, B., 2007. Broad thermo-barometric evolution of the Eastern Goldfields Superterrane. In: Bierlien, F.P., Knox-Robinson, C.M. (Eds.), Proceedings of Geoconferences (WA) Inc. Kalgoorlie '07 Conference, Geoscience Australia Record, vol. 2007/14, pp. 33–38.

Hamiel, Y., Liu, Y., Lyakhovsky, V., Ben-Zion, Y., Lockner, D., 2004. A visco-elastic damage model with applications to stable and unstable fracturing. Geophysical Journal International 159, 1155–1165.

Hancock, P.L., Chalmers, R.M.L., Altunel, E., Çakir, Z., 1999. Travitonics: using travertines in active fault studies. Journal of Structural Geology 21, 903–916.

Hardebeck, J.L., Nazareth, J.J., Hauksson, E., 1998. The static stress change triggering model: Constraints from two southern California aftershock sequences. Journal of Geophysical Research 103, 24427–24437.

Hedenquist, J.W., Lowenstern, J.B., 1994. The role of magmas in the formation of hydrothermal ore deposits. Nature 370, 519–527.

Hickman, S.H., Evans, B., 1987. Influence of geometry upon crack healing rate in calcite. Physics and Chemistry of Minerals 15, 91–102.

Hill, D.P., Reasenberg, P.A., Michael, A., Arabaz, W.J., Beroza, G., Brumbaugh, D., Brune, J.N., Castro, R., Davis, S., dePolo, D., Ellsworth, W.L., Gomberg, J., Harmsen, S., House, L., Jackson, S.M., Johnston, M.J.S., Jones, L., Keller, R., Malone, S., Munguia, L., Nava, S., Pechmann, J., Sanford, C.A., Simpson, R.W., Smith, R.B., Stark, M., Stickney, M., Vidal, A., Walter, S., Wong, V., Zollweg, J., 1993. Seismicity remotely triggered by the Magnitude 7.3 Landers, California, Earthquake. Science 260, 1617–1623.

Hill, D.P., Johnston, M.J.S., Langbein, J.O., 1995. Response of Long Valley caldera to the Mw = 7.3 Landers, California, earthquake. Journal of Geophysical Research 100, 12985–13005.

Hiramatsu, Y., Honma, H., Saiga, A., Furumoto, M., Ooida, T., 2005. Seismological evidence on characteristic time of crack healing in the shallow crust. Geophysical Research Letters 32, L09304. doi:10.1029/2005GL022657.

Hitzman, M.W., Redmond, P.B., Beaty, D.W., 2002. The carbonate-hosted Lisheen Zn–Pb–Ag deposit, County Tipperary, Ireland. Economic Geology 97, 1627–1655.

Hurst, T., Bannister, S., Robinson, R., Scott, B., 2008. Characteristics of three recent earthquake sequences in the Taupo Volcanic Zone, New Zealand. Tectonophysics 452, 17–28.

Husen, S., Taylor, R., Smith, R.B., Healser, H., 2004. Changes in geyser eruption behavior and remotely triggered seismicity in Yellowstone National Park produced by the 2002 M 7.9 Denali fault earthquake, Alaska. Geology 32, 537–540.

Imber, J., Holdsworth, R.E., Butler, C.A., Strachan, R.A., 2001. A reappraisal of the Sibson–Scholz fault zone model: the nature of the frictional to viscous ("brittle-ductile") transition along a long-lived, crustal-scale fault, Outer Hebrides, Scotland. Tectonics 20, 601–624.

Irwin, W.P., Barnes, I., 1980. Tectonic relations of carbon dioxide discharges and earthquakes. Journal of Geophysical Research 85, 3115–3121.

Jenatton, L., Guiguet, R., Thouvenot, F., Daix, N., 2007. The 16000-event 2003–2004 earthquake swarm in Ubaye (French Alps). Journal of Geophysical Research 112, B11304,. doi:10.1029/2006JB004878.

Johnson, K.M., Segall, P., 2004. Viscoelastic earthquake cycle models with deep stress-driven creep along the San Andreas fault system. Journal of Geophysical Research 109, 1–19. doi:10.1029/2004JB003096. B10403.

Kase, Y., Kuge, K., 1998. Numerical simulations of spontaneous rupture processes on two non-coplanar faults: the effect of geometry on fault interaction. Geophysical Journal International 135, 911–922.

Katz, O., Reches, Z., 2004. Microfracturing, damage, and failure of brittle granites. Journal of Geophysical Research 109, B01206. doi:10.1029/2002JB001961.

Kay, M.A., Main, I.G., Elphick, S.C., Ngwenya, B.T., 2006. Fault gouge diagenesis at shallow burial depth: solution-precipitation reactions in well-sorted and poorly sorted powders of crushed sandstone. Earth and Planetary Science Letters 243, 607–614.

Kilb, D., Rubin, A.M., 2002. Implications of diverse fault orientations imaged in relocated aftershocks of the Mount Lewis, M_L 5.7, California, earthquake. Journal of Geophysical Research 107, 1–17. doi:10.1029/2001JB000149.

Kim, Y.-S., Peacock, D.C.P., Sanderson, D.J., 2003. Fault damage zones. Journal of Structural Geology 26, 503–517.

King, G.C., Stein, R.S., Lin, J., 1994. Static stress changes and the triggering of earthquakes. Bulletin of the Seismological Society of America 84, 567–585.

Knipe, R.J., 1989. Deformation mechanisms – recognition from natural tectonites. Journal of Structural Geology 11, 127–146.

Koerner, A., Kissling, E., Miller, S.A., 2004. A model of deep crustal fluid flow following the Mw = 8.0 Antofagasta, Chile, earthquake. Journal of Geophysical Research 109, 1–11. doi:10.1029/2003JB002816. B06307.

Kolb, J., Rogers, A., Meyer, F.M., Vennemann, T.W., 2004. Development of fluid conduits in the auriferous shear zones of the Hutti Gold Mine, India: evidence for spatially and temporally heterogeneous fluid flow. Tectonophysics 378, 65–84.

Liu, J., Sieh, K., Hauksson, K., 2003. A structural interpretation of the aftershock "cloud" of the 1992 M_w 7.3 Landers earthquake. Bulletin of the Seismological Society of America 93, 1333–1344.
Lyakhovsky, V., Ben-Zion, Y., Agnon, A., 1997. Distributed damage, faulting, and friction. Journal of Geophysical Research 102, 27635–27649.
Main, I.G., 2000. A damage mechanics model for power-law creep and earthquake aftershock and foreshock sequences. Geophysical Journal International 142, 151–161.
Mancktelow, N.S., Grujic, D., Johnson, E.L., 1998. An SEM study of porosity and grain boundary microstructure in quartz mylonites, Simplon fault zone, central Alps. Contributions to Mineralogy and Petrology 131, 71–85.
Manning, C.E., Ingebritsen, S.E., 1999. Permeability of the continental crust: implications of geothermal data and metamorphic systems. Reviews of Geophysics 37, 127–150.
McCaffrey, K.J.W., Johnston, J.D., 1996. Fractal analysis of a mineralised vein deposit: Curraghinalt gold deposit, County Tyrone. Mineralium Deposita 31, 52–58.
McCaig, A.M., Knipe, R.J., 1990. Mass-transport mechanisms in deforming rocks: recognition using microstructural and microchemical criteria. Geology 18, 824–827.
McCuaig, T.C., Kerrich, R., 1998. P–T–t-deformation-fluid characteristics of lode gold deposits: evidence from alteration systematics. Ore Geology Reviews 12, 381–453.
Micklethwaite, S., 2007. The significance of linear trends and clusters of fault-related mesothermal lode gold mineralization. Economic Geology 102, 1157–1164.
Micklethwaite, S., 2008. Optimally oriented "fault-valve" thrusts: Evidence for aftershock-related fluid pressure pulses? Geochemistry, Geophysics. Geosystems 9, 1–10. doi:10.1029/2007GC001916. Q04012.
Micklethwaite, S., 2009. Mechanisms of faulting and permeability enhancement during epithermal mineralisation: Cracow goldfield, Australia. Journal of Structural Geology 31 (3), 288–300.
Micklethwaite, S., Cox, S.F., 2004. Fault-segment rupture, aftershock-zone fluid flow, and mineralization. Geology 32, 813–816.
Micklethwaite, S., Cox, S.F., 2006. Progressive fault triggering and fluid flow in aftershock domains: examples from mineralized Archaean fault systems. Earth and Planetary Science Letters 250, 318–330.
Miller, S.A., Colletini, C., Chiaraluce, L., Cocco, M., Barchi, M., Kaus, B.J.P., 2004. Aftershocks driven by a high-pressure CO_2 source at depth. Nature 427, 724–727.
Montési, L.G., 2004. Controls of shear zone rheology and tectonic loading on postseismic creep. Journal of Geophysical Research 109, 1–18. doi:10.1029/2003JB002925. B10404.
Muchez, P., Heijlen, W., Banks, D., Blundell, D., Boni, M., Grandia, F., 2005. Extensional tectonics and the timing and formation of basin-hosted deposits in Europe. Ore Geology Review 27, 241–267.
Muntean, J.L., Coward, M.P., Tarnocai, C.A., 2007. Reactivated Paleozoic normal faults: Controls on the formation of Carlin-type gold deposits in north-central Nevada. Geological Society London Special Publication 272, 571–589.
Nevada Bureau of Mines and Geology, Bulletin 111, 2002. In: Thompson, T.B., Teal, L., Meeuwig, R.O. (Eds.), Gold deposits of the North Carlin Trend. University of Nevada, Reno.
Nortje, G.S., Rowland, J.V., Spörli, K.B., Blenkinsop, T.G., Rabone, S.D.C., 2006. Vein deflections and thickness variations of epithermal quartz veins as indicators of fracture coalescence. Journal of Structural Geology 28, 1396–1405.
Oliver, N.H.S., 2001. Linking of regional and hydrothermal systems in the mid-crust by shearing and faulting. Tectonophysics 335, 147–161.
Pachell, M.A., Evans, J.P., 2002. Growth, linkage, and termination processes of a 10-km-long strike-slip fault in jointed granite: the Gemini fault zone, Sierra Nevada, California. Journal of Structural Geology 24, 1903–1924.
Peach, C.J., Spiers, C.J., 1996. Influence of crystal plastic deformation on dilatancy and permeability development in synthetic rock salt. Tectonophysics 256, 101–128.
Peacock, D.C.P., 1991. Displacements and segment linkage in strike-slip fault zones. Journal of Structural Geology 13, 1025–1035.
Peacock, D.C.P., Sanderson, D.J., 1991. Displacements, segment linkage and relay ramps in normal fault zones. Journal of Structural Geology 13, 721–733.
Pollitz, F.F., Sacks, S., 2002. Stress triggering of the 1999 Hector Mine earthquake by transient deformation following the 1992 Landers earthquake. Bulletin of the Seismological Society of America 92, 1487–1496.
Reasenberg, P., Simpson, R.W., 1992. Response of regional seismicity to the static stress change produced by the Loma Prieta earthquake. Science 255, 1687–1690.
Reches, Z., Lockner, D.A., 1994. Nucleation and growth of faults in brittle rocks. Journal of Geophysical Research 99, 18159–18173.
Reyners, M., Eberhart-Phillips, D., Stuart, G., 2007. The role of fluids in lower-crustal earthquakes near continental rifts. Nature 446, 1075–1078.
Richards, J.P., 2003. Tectono-magmatic precursors for Porphyry Cu-(Mo–Au) deposit formation. Economic Geology 98, 1515–1533.
Ridley, J.R., Diamond, L.W., 2000. Fluid chemistry of orogenic lode gold deposits and implications for genetic models. Reviews in Economic Geology 13, 141–162.
Robert, F., Poulsen, K.H., 1997. World-class gold deposits in Canada: an overview. Australian Journal of Earth Sciences 44, 329–351.
Robert, F., Boullier, A.-M., Firdaous, K., 1995. Gold-quartz veins in metamorphic terranes and their bearing on the role of fluids in faulting. Journal of Geophysical Research 100, 12,861–12,881.
Robert, F., Poulsen, K.H., Cassidy, K.F., Hodgson, C.J., 2005. Gold metallogeny of the Superior and Yilgarn Cratons. In: Economic Geology 100th Anniversary Volume, pp. 1001–1033.
Roberts, S., Sanderson, D.J., Gumiel, P., 1999. Fractal analysis and percolation properties of veins. Geological Society Special Publication 155, 7–16.
Rojstaczer, S., Wolf, S., Michel, R., 1995. Permeability enhancement in the shallow crust as a cause of earthquake-induced hydrological changes. Nature 373, 237–239.
Rolandone, F., Bürgmann, R., Nadeau, R.M., 2004. The evolution of the seismic–aseismic transition during the earthquake cycle: constraints from the time-dependent depth distribution of aftershocks. Geophysical Research Letters 31, 1–4. doi:10.1029/2004GL021379. L23610.
Roman, D.C., Cashman, K.V., 2006. The origin of volcano-tectonic earthquake swarms. Geology 34, 457–460. doi:10.1130/G22269.1.
Rybacki, E., Wirth, R., Dresen, G., 2008. High-strain creep of feldspar rocks: implications for cavitation and ductile failure in the lower crust. Geophysical Research Letters 35, L04304. doi:10.1029/2007GL032478.
Sanderson, D.J., Roberts, S., Gumiel, P., Greenfield, C., 2008. Quantitative analysis of Tin- and Tungsten-bearing sheeted vein systems. Economic Geology 103, 1043–1056.
Savage, J.C., Svarc, J.L., Prescott, W.H., 2003. Near-field postseismic deformation associated with the 1992 Landers and 1999 Hector Mine, California, earthquakes. Journal of Geophysical Research 108, 1–10. doi:10.1029/2002JB002330. B2432.
Scholz, C.H., 2002. The Mechanics of Earthquakes and Faulting. Cambridge University Press, New York.
Schwartz, S.Y., Rokosky, J.M., 2007. Slow-slip events and seismic tremor at circum-pacific subduction zones. Reviews of Geophysics 45, RG3004,. doi:10.1029/2006RG000208.
Shapiro, S.A., Patzig, R., Rothert, E., Rindschwenter, J., 2003. Triggering of seismicity by pore-pressure perturbations: permeability-related signatures of the phenomenon. Pure and Applied Geophysics 160, 1051–1066.
Sheldon, H.A., Micklethwaite, S., 2007. Damage and permeability around faults: implications for mineralization. Geology 34, 903–906. doi:10.1130/G23860A.1.
Shigematsu, N., Fujimoto, K., Ohtani, T., Shibazaki, B., Tomita, T., Tanaka, H., Miyashita, Y., 2009. Localisation of plastic flow in the mid-crust along a crustal-scale fault: insight from the Hatagawa Fault Zone, NE Japan. Journal of Structural Geology 31, 601–614.
Shipton, Z.K., Cowie, P.A., 2001. Damage zone and slip-surface evolution over μm to km scales in high-porosity Navajo sandstone, Utah. Journal of Structural Geology 23, 1825–1844.
Sibson, R.H., 1983. Continental fault structure and the shallow earthquake source. Journal of the Geological Society of London 140, 741–767.
Sibson, R.H., 1985. Stopping of earthquake ruptures at dilational fault jogs. Nature 316, 248–250.
Sibson, R.H., 1987. Earthquake rupturing as a mineralizing agent in hydrothermal systems. Geology 15, 701–704.
Sibson, R.H., 1989. Earthquake faulting as a structural process. Journal of Structural Geology 11, 1–14.
Sibson, R.H., 2001. Seismogenic framework for hydrothermal transport and ore deposition. Reviews in Economic Geology 14, 25–50.
Sibson, R.H., Robert, F.K., Poulsen, K.H., 1988. High-angle reverse faults, fluid--pressure cycling, and mesothermal gold-quartz deposits. Geology 16, 551–555.
Simmons, S.F., Brown, K.L., 2007. The flux of gold and related metals through a volcanic arc, Taupo Volcanic Zone, New Zealand. Geology 35, 1099–1102.
Simmons, S.F., White, N.C., John, D.A., 2005. Geological characteristics of epithermal precious and base metal deposits. In: Economic Geology 100th Anniversary Volume, pp. 485–522.
Smith, S.A.F., Colletini, C., Holdsworth, R.E., 2008. Recognizing the seismic cycle along ancient faults: CO2-induced fluidization of breccias in the footwall of a sealing low-angle normal fault. Journal of Structural Geology 30, 1034–1046.
Soliva, R., Benedicto, A., 2005. Geometry, scaling relations and spacing of vertically restricted normal faults. Journal of Structural Geology 27, 317–325.
Soliva, R., Schultz, R.A., 2008. Distributed and localized faulting in extensional settings: insight from the Ethiopian Rift-Afar transition area. Tectonics 27, 1–19. doi:10.1029/2007TC002148. TC2003.
Souley, M., Homand, F., Pepa, S., Hoxha, D., 2001. Damage-induced permeability changes in granite: a case example at the URL in Canada. International Journal of Rock Mechanics and Mining Sciences 38, 297–310.
Steefel, C.I., DePaolo, D.J., Lichtner, P.C., 2005. Reactive transport modeling: an essential tool for a new research approach for the Earth sciences. Earth and Planetary Science Letters 240, 539–558.
Stein, R.S., King, G.C.P., Lin, J., 1992. Change in failure stress on the Southern San Andreas Fault System caused by the 1992 magnitude = 7.4 Landers earthquake. Science 258, 1328–1331.
Stein, R.S., Barka, A.A., Dieterich, J.H., 1997. Progressive failure on the North Anatolian fault since 1939 by earthquake stress triggering. Geophysical Journal International 128, 594–604.
Tadokoro, K., Ando, M., 2002. Evidence for rapid fault healing derived from temporal changes in S wave splitting. Geophysical Research Letters 29, 1–4. doi:10.1029/2001GL013644.
Templeton, D.C., Dreger, D.S., 2006. Non-double-couple earthquakes in the Long Valley volcanic region. Bulletin of the Seismological Society of America 96, 69–79.

Tenthorey, E., Fitz Gerald, J., 2006. Feedbacks between deformation, hydrothermal reaction and permeability evolution in the crust: experimental insights. Earth and Planetary Science Letters 247, 117–129.
Tenthorey, E., Cox, S.F., Todd, H.F., 2003. Evolution of strength recovery and permeability during fluid-rock reaction in experimental fault zones. Earth and Planetary Science Letters 206, 161–172.
Toda, S., Stein, R.S., Sagiya, T., 2002. Evidence form the AD 2000 Izu Islands earthquake swarm that stressing rate governs seismicity. Nature 419, 58–61.
Torkler, L., McKay, D., Hobbins, J., 2006. Geology and exploration of the Favona Au–Ag deposit, Waihi, Hauraki goldfield. The Australasian Institute of Mining and Metallurgy, Monograph 25, 1–6.
Townend, J., Zoback, M.D., 2000. How faulting keeps the crust strong. Geology 28, 399–402.
Trepmann, C.A., Stöckhert, B., 2003. Quartz microstructures developed during non-steady state plastic flow at rapidly decaying stress and strain rate. Journal of Structural Geology 25, 2035–2051.
Utsu, T., Ogata, Y., Matsuura, R.S., 1995. The centenary of the Omori formula for a decay law of aftershock activity. Journal of Physics of the Earth 43, 1–33.
Uysal, I.T., Feng, Y., Zhao, J.-X., Altunel, E., Weatherley, D., Karabacak, V., Cengiz, O., Golding, S.D., Lawrence, M.G., Collerson, K.D., 2007. U-series dating and geochemical tracing of late Quaternary travertine in co-seismic fissures. Earth and Planetary Science Letters 257, 450–462.
Voisin, C., Cotton, F., Carli, S.D., 2004. A unified model for dynamic and static stress triggering of aftershocks, antishocks, remote seismicity, creep events and multisegmented rupture. Journal of Geophysical Research 109, 1–12. doi:10.1029/2003JB002886. B06304.
Waite, G.P., Smith, R.B., 2002. Seismic evidence for fluid migration accompanying subsidence of the Yellowstone caldera. Journal of Geophysical Research 107 (B9), 2177,. doi:10.1029/2001JB000586.
Walsh, J.J., Bailey, W.R., Childs, C., Nicol, A., Bonson, C.G., 2003. Formation of segmented normal faults: a 3-D perspective. Journal of Structural Geology 25, 1251–1262.
Wells, D.L., Coppersmith, K.J., 1994. New empirical relationships among magnitude, rupture length, rupture width, rupture area, and surface displacement. Bulletin of the Seismological Society of America 84, 974–1002.
Weinberg, R.F., Hodkiewicz, P.F., Groves, D.I., 2004. What controls gold distribution in Archean terranes? Geology 32, 545–548.
Weinberg, R.F., van der Borgh, P., Bateman, R.J., Groves, D.I., 2005. Kinematic history of the Boulder–Lefroy shear zone system and controls on associated gold mineralization, Yilgarn craton, Western Australia. Economic Geology 100, 1407–1426.
Wesnousky, S.G., 1988. Seismological and structural evolution of strike-slip faults. Nature 335, 340–343.
Wesnousky, S.G., 2006. Predicting the endpoints of earthquake ruptures. Nature 444, 358–360. doi:10.1038/nature05275.
Wilkinson, J.J., Johnston, J.D., 1996. Pressure fluctuations, phase separation, and gold precipitation during seismic fracture propagation. Geology 24, 395–398.
Woodcock, N.H., Dickson, J.A.D., Tarasewicz, J.P.T., 2007. Transient permeability and reseal hardening in fault zones: evidence from dilation breccia textures. In: Geological Society, London, Special Publications, vol. 270, pp. 43-53.